

**Design and Construction of a  
Laser Display and a new  
Electro-Optic Modulator**

Anna Fragemann

Master's Thesis  
Lund Reports on Atomic Physics, LRAP 274  
LTH, May 2001

## **Abstract**

In this thesis the technologies necessary for development of Laser TVs and Laser projectors are examined. A vector graphics system is built and a fast electro-optic modulator is constructed.

Different techniques, which can be used to build laser displays, are compared and a scanned, vector graphics projector is constructed. The main components in the set-up are two galvanometer scanners, an acousto-optic intensity modulator and the driver electronics. This system can display figures and texts.

In order to develop vector graphics systems into raster scanned displays, the set-up has to be modified with a polygon mirror and a faster intensity modulator. Polygon mirrors exist, however a new modulator, operating in the visible region, had to be constructed. An electro-optic modulator, using the new material RTP was designed and tested. The highest modulation frequency used was 250 MHz, but frequencies of up to the order of GHz should be possible.

## **Acknowledgements**

I would like to thank Fredrik Laurell, my supervisor at KTH, for the opportunity to work with this thesis in his group and for helping and supporting me during my work.

I would also like to thank Valdas Pasiskevicius for helping me so many hours in the lab, while I was building the modulator, for all the discussions and for all his answers.

Thanks also to my supervisor and examiner at LTH, Stefan Kröll.

Thanks to Jenni Nordborg and Stefan Holmgren, who were sharing the room with me, for their help, Andreas Gaarder for playing good music and the rest of the group for answering questions and letting me borrow equipment.

Moreover I am thankful to Rune Persson for helping me with the construction of the display's set-up.

Thanks to Arvid Brodin for writing most of the computer code and to Magnus Pihl for constructing the DAC board.

Finally, I would like to thank my family and my boyfriend Mattias for their love and support.

# Table of Contents

Abstract	i
Acknowledgments	iii
<b>1. Introduction</b>	<b>1</b>
<b>2. The Laser Projector – Theory</b>	<b>2</b>
2.1 Television Sets and Projectors	2
2.1.1 How Does a Cathode Ray Tube Work?	2
2.1.2 The Liquid Crystal Display	4
2.1.3 The Plasma Display	6
2.2 Picture Scan Rate and Picture Definition	6
2.3 Additive and Subtractive Colours	7
2.4 The Colour Gamut	7
2.5 Today's TVs/Projectors in Comparison with Future Laser- TVs/Projectors	9
2.6 Comparison of Projector and TV Techniques	9
2.6.1 The Scanning System	9
2.6.2 The Matrix Based System	10
2.6.3 The Line Array System	11
2.7 Conclusion	11
<b>3. The Setup</b>	<b>13</b>
3.1 The Components	13
3.1.1 The Laser	13
3.1.2 The Scanners and Servo Cards	14
3.1.3 The Power Supply and Function Generator	15
3.2 The First Experiments	15
3.3 Improvements	16
3.3.1 The DAC Board	16
3.3.2 The Software	17
3.3.3 The Modulator	18
3.3.3.1 Acousto-Optic Modulator	18
3.3.3.2 Electro-Optic Modulator	19
3.3.4 Using the AOM for Blanking	19
3.4 Possibilities to Develop the Raster Scanned Projection System	21
<b>4. The Electro-Optic Modulator – Theory</b>	<b>23</b>
4.1 Anisotropic Crystals	23
4.2 The $\text{KTiOPO}_4$ Isomorphs	24
4.3 The Electro-Optic Effect	25
4.4 The Principle for an Electro-Optic Modulator	28

<b>5</b>	<b>The First Electro-Optic Modulator – Calculation, Construction and Testing</b>	<b>31</b>
5.1	Absorption Coefficient for the KTP Isomorphs	31
5.1.1	How to Determine Absorption Coefficients	31
5.1.2	The Measurements Done for Determination of Absorption Coefficients	33
5.2	Construction of the EOM	34
5.3	First Experiments	35
5.4	Improvements for the EOM	37
<b>6</b>	<b>The Modified EOM</b>	<b>38</b>
6.1	Construction of the Modified EOM	38
6.2	Temperature Measurement	38
6.3	High Frequency Measurement	39
6.3.1	Determination of the Transfer Function	40
6.3.2	Determination of the Crystal's Impedance	41
6.3.3	The EOM's Ability to Modulate at Different Frequencies	43
6.3.4	The High Speed EOM	46
6.4	Summary of the EOMs	47
<b>7.</b>	<b>Summary</b>	<b>48</b>
<b>8.</b>	<b>References</b>	<b>49</b>

# 1 Introduction

The aim of this master's thesis was to build a simple Laser projector and examine the possibilities to develop it into a more advanced working Laser TV. As a part of the projector a new type of electro-optic intensity modulator was constructed.

The main parts of a Laser projector are the light source, the projection technique, the intensity modulator and the control electronics. Before the construction could start, the projection technique had to be chosen, as it has a great influence on the choice of the other components. Three different techniques can be used for projecting a picture on the screen. The first technique is a scanning system, which reminds of the cathode ray tube (CRT) and the second system is matrix based, where the construction is similar to a liquid crystal display (LCD). Finally, a mixture of these two techniques exists, which is called the line array system. After comparison of these techniques the scanning system was chosen for this project.

The first sub-goal was to build a system, which is able to draw vector graphics. This means that the laser beam is not scanned across the whole screen, but only draws the picture's contours. For this purpose two scanners are needed – one for vertical and one for horizontal deflection. The scanners are deflected by the control electronics, which consist of several circuit boards. The control electronics is also connected to a computer, which by means of a program calculates the points the picture consists of.

Using these components it is possible to draw closed figures, but in order to write letters or draw other more complicated pictures, it must be possible to block the laser beam. In order to avoid certain lines, connecting two points, to be visible on the screen, an acousto-optic intensity modulator is used.

However, it would require many modifications to extend this system into a raster scanned full-picture projector. The galvanometer scanners only work at frequencies less than 600 Hz, which means that the horizontal scanner has to be replaced by a polygon mirror, which can deflect the laser beam with up to 30-40 kHz. These scanners are unfortunately expensive and as it was impossible to borrow one, the expansion of the projector could not continue in this direction.

Instead work was focussed on another component, which also had to be improved before it is possible to build a complete raster scanned system. The acousto-optic modulator is fast enough to block the laser beam when vector graphics is drawn. However, a scanning full-picture projector needs intensity modulation with the speed of approximately 30 MHz, which is easier to achieve with electro-optic modulators.

As the final part in my project I designed and constructed an electro-optic intensity modulator using the new material RTP. Measurements were made in order to determine its ability to modulate light at high frequencies and to determine its temperature sensitivity. The result was that this modulator is fast enough for usage in Laser TVs. The highest frequency, which was tested, was 250 MHz, but frequencies as high as some GHz should be possible.

## 2 The Laser Projector – Theory

### 2.1 Television Sets and Projectors

The general aim of TVs and projectors is to convert the received electrical signals into optical images on a screen. The techniques used for these two systems are very similar. The biggest difference is the viewer's position with respect to the device and the picture.

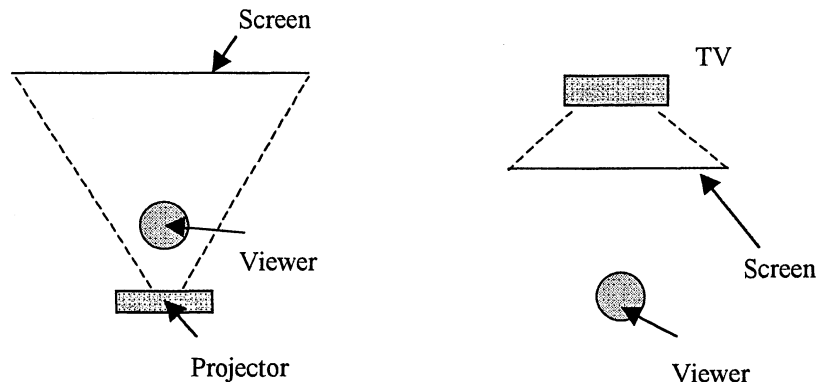


**Figure 2.1** The main difference between Projectors and TVs.

In general, projectors produce larger pictures than TVs, which is the main reason why they are chosen, when something is shown to a large group.

The still predominant technique used for televisions is the cathode ray tube (CRT). But TVs using liquid crystal displays (LCD) are becoming common as well.

#### 2.1.1 How Does a Cathode Ray Tube Work?

The interior components of a cathode ray tube can roughly be divided into two parts. The first is responsible for generating an electron beam and the second part is responsible for deflecting and focusing this beam. In Figure 2.2 the components for the electron beam generation are shown. Among other components a cathode, an anode and a control electrode can be seen. The electrical input signal is connected to the control electrode and causes the potential to vary about a mean level. When the signal to the control electrode goes negative, the intensity of the electron beam decreases. A less negative signal on the other hand results in a more intense electron beam.

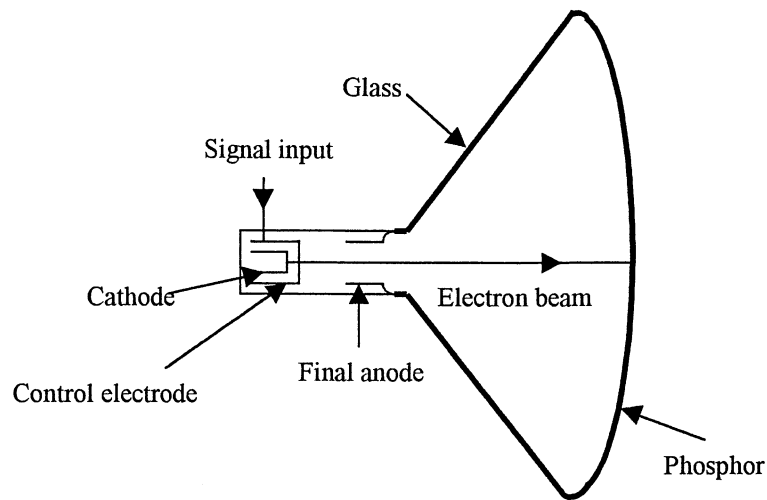


**Figure 2.2** Generation of the Electron Beam.

The screen is made of a phosphor, which emits light when electrons hit it. The intensity of a point on the screen is proportional to the amount of electrons bombarding it. Thus an intense electron beam results in a bright spot, while a weak electron beam gives a less bright spot on the screen. In other words by varying the input signal to the control electrode the brightness of each spot on the screen can easily be controlled.

In order to get a complete picture on the screen, the beam has to be scanned over the whole screen. In general the beam starts in the top left corner and moves in a horizontal line to the right hand side across the screen. Having reached the right hand side it is quickly deflected back to the left. This movement is called flyback and is initiated by an electrical signal called the horizontal sync pulse. At the same time it is also deflected downwards so that the next horizontal line can be scanned. After reaching the bottom right corner the electron beam has to return to the top left corner of the screen in order to begin a complete, new scanning process. The electrical signal initiating this return is called the vertical sync pulse.

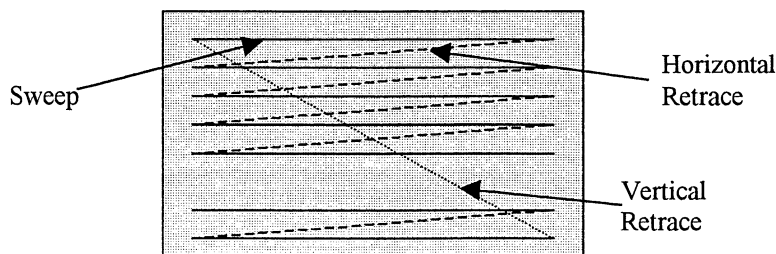


**Figure 2.3** The Television Frame Scan.



The deflection of the electron beam can be achieved both electrically and magnetically. As magnetic deflection permits a shorter tube this technique is preferred and most common. A magnetic field exerts a force on the electrons in a beam and can thus be used to deflect the whole beam. The electron beam has to be deflected at a constant velocity in order to get a regular picture on the screen. Hence, the magnetic field must be built up steadily. This in turn favours the use of electromagnetic fields instead of permanent magnetic fields. The current to the coils, used to generate the magnetic field, can be controlled in the desired manner. For example sending the horizontal sync pulse initiates the flyback, and the vertical sync pulse initiates the return to the top left corner.

Besides deflecting the electron beam, it also has to be focussed, which is usually done either electrically or magnetically.

### 2.1.2 The Liquid Crystal Display

The biggest disadvantage with CRT screens is their bulky size. Due to the difficulties of deflecting the electron beam by large angles, they cannot be made flatter. Thus, the electron beam has to be replaced by another technique, which can both address the pixels on the screen and create light in each pixel. This can be achieved by using digital addressing, which is done in liquid crystal displays (LCDs), instead of the analogue approach.

Each pixel consists of two polarisers, as shown in Figure 2.4. Between them the LC (liquid crystal) material is assembled in such a way that the LC molecules undergo a 90° twist from the top to the bottom plate. Incident polarised light will undergo a 90° rotation when passing through the liquid crystal and will thus pass through the second polariser. The cell is transmissive.

On the other hand, if voltage is applied to the liquid crystal, the molecules will align with the field. The incident light will not be rotated and will therefore be absorbed by the second polariser. In this case the cell is opaque.

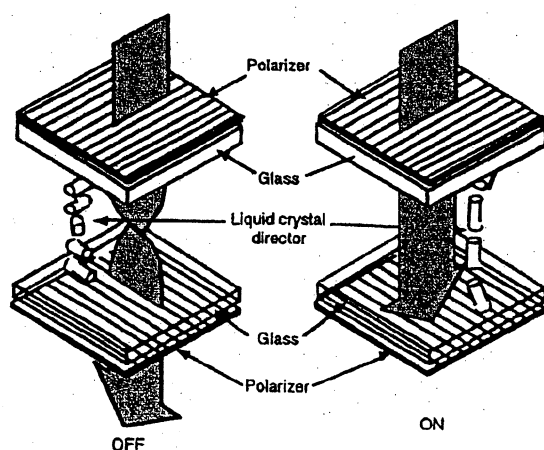
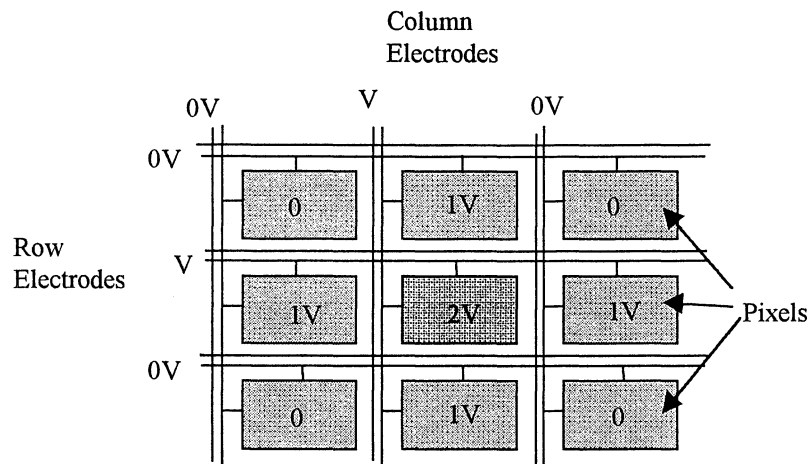


Figure 2.4 The Principle of a LCD cell.<sup>1</sup>

Two different techniques to address the pixels exist, either passive or active matrices can be used. Passive matrices consist of row and column electrodes. By applying appropriate voltages to the electrodes, each pixel can be addressed as can be seen in Figure 2.5. To display a whole picture, the row electrodes are addressed sequentially. At the same time, appropriate voltages are applied to the column electrodes, which produces the image.



**Figure 2.5** The Passive matrix LCD. Addressing the centre pixel.

In order to give clear images, the electro-optic function describing the transmissivity in relation to the applied voltage should be as steep as possible. In the passive matrix technique however the electro-optic curve has a limited slope.

Instead a different technique was proposed to increase the slope of the curve. In Active Matrix Liquid Crystal Displays (AMLCDs) a solid state circuit device with strong non-linearities is inserted. Either a two-terminal device as a diode or a three-terminal device as a transistor can be used. Currently, however, thin-film transistors are preferred to thin-film diodes because they provide increased isolation between the control and the signal lines and are less susceptible to manufacturing tolerances.

The LCD cells do not generate light but only modulate it. Thus some sort of lighting is needed. Initially, LCD screens were using the reflective mode, but the result was an unsatisfactory picture quality. Now, the backlighting technique is dominant and the lamps used are cold cathode fluorescent lamps. These consist of a glass, which is coated with phosphor and filled with a low-pressure gas. When high voltage is applied, the gas is ionised and a current flows, which causes the emission of UV-light. This light excites the phosphor on the inside walls of the glass.<sup>1</sup>

### 2.1.3 The Plasma Display

A third rather new technique for screens is the plasma display (PDP). These screens are flat as the LCD screen systems and are very attractive for large display areas. A pixel in a plasma display consists of a small pocket, which is made up by two glass panels. In the space between the glass panels, electrodes are situated and moreover the pockets contain inert gas, typically a blend of helium and xenon. When the electrodes are charged an electric current passes through the gas and ionises it. Thus the gas changes to the state of plasma, which refers to an electrically neutral mixture of electrons, positively and negatively charged ions and gas molecules which are not ionised. The ionised gas emits ultraviolet light, which in turn reacts with red, green and blue phosphor in each pixel to produce visible light.

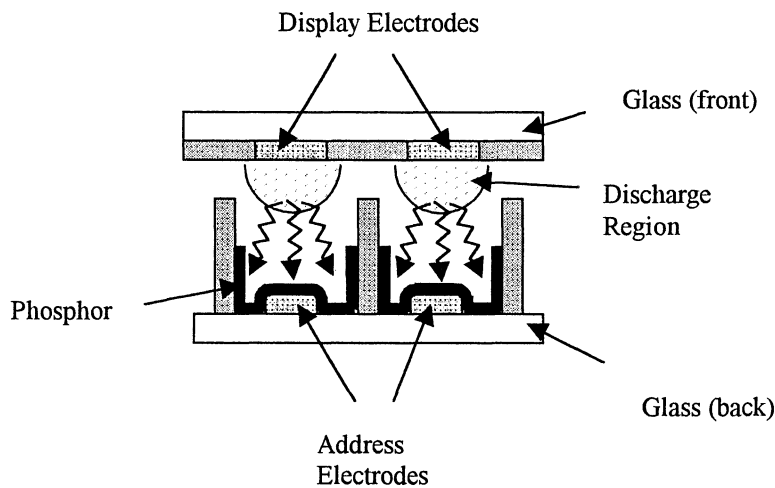


**Figure 2.6** Two Plasma Display pixels.

In PDPs the signal must be arranged and applied in the same way as in LCDs. One row of cells at the time has to be addressed. Two different types exist, the alternating current and the direct current displays. In both cases pulses of voltage are applied to the cells, but in the first case the pulses have alternating polarity and in the second they are always of the same polarity. In comparison the direct current displays are heavier than alternating current displays, have shorter life span and are less efficient, generating excessive heat during the operation.<sup>1</sup>

## 2.2 Picture Scan Rate and Picture Definition

In CRTs one complete scanning of the screen results in the reproduction of one single picture. If the amount of pictures being scanned per time interval, the so-called picture scan rate, is too low, the movements in the films will not be smooth enough. Instead the

picture sequence will resemble a stop-and-go film. Another difficulty is that the phosphors have a rather low persistence. As a consequence the pictures will fade away between the scans, which might cause flickering.

The picture rate must thus be sufficiently high so that the human eye will override the flickering and will be able to merge the picture series to smooth motion. The minimum picture rate making this possible is approximately 35 to 50 picture per second.

The picture definition represents the resolution of the television. It is determined by the smallest possible element in a picture, which in a scanning system is set by the number of vertical and horizontal lines in a frame and in a LCD system by the pixel size.

There are several different systems, which are characterised by their different resolutions, which means the different numbers of lines (vertical lines x horizontal lines)

PAL (Phase Alternation by Line):	720 x 576
NTSC (National Television Standards Committee):	640 x 480
SVGA (Super Video Graphics Array):	800 x 600
XGA (Extended Graphics Array):	1024 x 768
HDTV (High Definition Television) :	1920 x 1080

Understandingly, the HDTV with three times more horizontal pixels than the NTSC standard TV has a much higher resolution and a larger picture.

## 2.3 Additive and Subtractive Colours

In colour CRTs three electron beams are needed, one beam for each of the colours red, green and blue. Three different phosphors have to be used as well, one for each colour. Thus each of the picture pixels is divided into three smaller, coloured pixels. Using these three colours almost every other colour can be produced. This is achieved as the human eye/brain instead of seeing three separate colours adds them together.

One might wonder why the primary colours, which are used in TVs, are red, green and blue and not red, yellow and blue as with paint. The reason is that light emitted by a lamp is an additive colour, whereas paint colours are subtractive colours. E.g. red paint appears to be red because it absorbs the green and the blue light. This is also the reason why a mixture of the three primary painting colours results in the colour black, while mixing the three primary colours of light, gives white light.

## 2.4 The Colour Gamut

All colours visible to the human eye can be arranged in a special chromaticity diagram, called the colour gamut defined by Pointer. In Figure 2.7 the primary colours are arranged along the border, starting with 400 nm at the left hand side bottom, across the top where 520 nm can be found, down to 700 nm at the right hand side bottom. Mixing different concentrations of these outer colours can reproduce all the colours inside the area.



Figure 2.7 The Colour Gamut.<sup>2</sup>

This diagram shows that the colours, which can be represented in colour CRTs, depend upon the choice of phosphors used to emit the primary colours. Each of the primary colours represents one corner in a triangle, where the resulting interior are the colours, which are possible to be displayed. As there are a limited number of available phosphors the triangle cannot cover the whole gamut. Actually less than half of the area can be covered when CRTs are used. The NTSC Standard results in a larger triangle but it is still smaller than the triangle, which can be achieved with lasers. This can be seen in Figure 2.8.

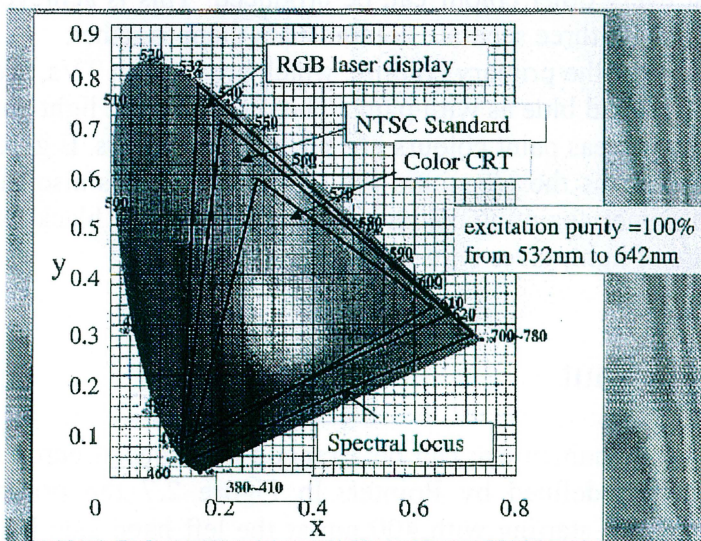


Figure 2.8 Comparison of different systems' colour quality.<sup>3</sup>

## 2.5 Today's TVs / Projectors in Comparison with Future Laser-TVs / Projectors

There are a couple of disadvantages with today's TV-sets: both with CRT TVs and liquid crystal displays.

The colour gamut of TVs is much smaller than the colour gamut the eye actually is sensitive to. The reason for this behaviour is the fluorescent screen, which is made out of three different phosphors. One phosphor is needed for each of the primary colours. But these phosphors only exist for certain colours and especially in the green domain the available phosphor (ca 565 nm) is not the one, which results in the largest triangle (ca 520 nm). Depending on the choice of lasers the colour gamut triangle for a laser TV has almost twice the area of today's TVs.

LCD TVs are rather ineffective in their usage of light. Only a part of the lamp's light is used to illuminate the screen, while the rest is lost in the other directions inside the TV. If lasers were used instead, less light would be wasted, because they selectively illuminate the screen.

As today's projector sets do not use collinear light the picture is only sharp at a certain distance and it is difficult to enlarge the picture. This is different when lasers are used. Because of their collinearity, the pictures' size can easily be enlarged and reduced, and the distance between the projector and the screen can be changed without loss of focus. Another consequence of collinearity is the possibility to project on round walls as for example in an observatory or flight simulation. When using laser projectors it is moreover very easy to change between different aspect ratios and resolutions.

Other advantages of Laser TVs are their long life span and their light weight. Moreover the lumens per electrical Watt for Laser TVs (10 lm/W) is much larger than that for CRTs (0.5 lm/W). Laser TVs will therefore consume less electrical power than other large screen displays, which will conserve an enormous amount of electrical energy.<sup>4</sup>

## 2.6 Comparison of Projector and TV Techniques

### 2.6.1 The Scanning System

This system works according to the same principles as the CRT, but instead of an electron beam, a laser spot is used. No phosphors are needed, as the laser itself is visible. An intensity modulated laser spot is scanned one line at a time across the screen, where the major challenges are the scanning and the modulation. The scanning has to be done mechanically. One technique to achieve this is to use a galvanometer scanner, which is rather slow, for the y-axis deflection and a fast rotating polygon mirror for the x-axis deflection. For the intensity modulation electro-optic modulators can be used.

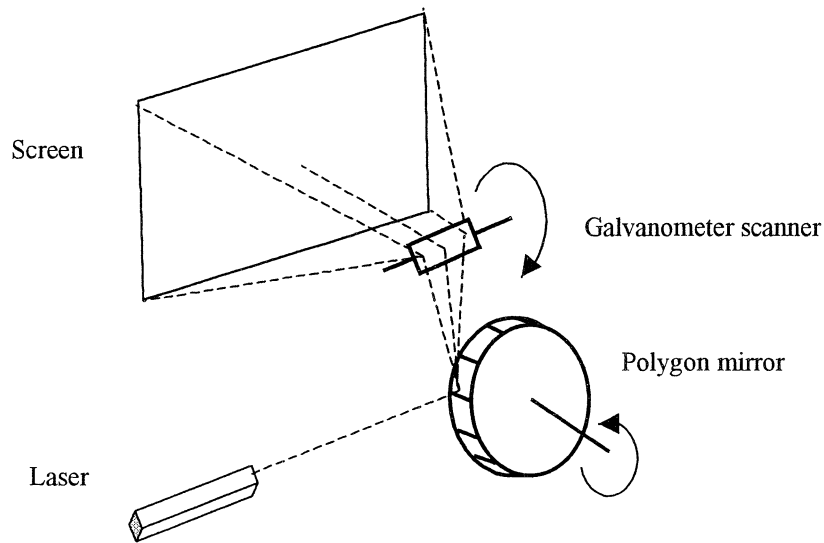


**Figure 2.9** The Scanning system.

The scanning system has the advantages that no pixel borders exist. Moreover the same construction can be used to display different resolutions and it is easy to change the size of the picture and the distance between wall and projector. Also the optical efficiency is very high, but on the other hand light is wasted during the retrace. Moreover this system demands a very high bandwidth, e.g. a HDTV, with 1920 vertical and 1080 horizontal lines and a picture scan rate of 100 pictures per second, will have a bandwidth of approximately 200 MHz. Another disadvantage is that the deflection and the modulation of the two axes require very good timing.

This approach to develop Laser TVs is tested at LDT, Laser Display Technology, in Germany, which is one of Schneider AG's research companies.

### 2.6.2 The Matrix Based System

The technique used in a matrix based projector was developed by Texas Instruments. In this system each spot on the screen can be associated with a physical pixel on a modulator array panel. Each pixel is addressable and operates by changing its transmissivity. One advantage of this system compared to the scanning system is the low bandwidth, which is required as each pixel is only updated once during each picture. Moreover the resolution is only limited by the architecture of the matrix. On the other hand the large number of pixels and video channels are a major disadvantage, for example it is difficult to get all the pixels working. Other disadvantages are the difficulty to convert between different resolutions and aspect ratios and the so-called screen door effect. This effect results in a grainy, pixelated picture, which occurs because the

horizontal and vertical spaces between the pixels block the light. The result is that only about 70% of the light shines through.

Moreover a large area has to be uniformly illuminated and as conventional lamps work satisfactory, lasers do not contribute to any major improvement. The main advantage of lasers – their very high brightness – cannot be translated into improved performance of the projector.

### 2.6.3 The Line Array System

The perfect solution would be a mixture of the scanning system and the matrix based system, with the possibility to combine the advantages of them both. This idea leads to the so-called line array system, which consists of a line array of physical pixels arranged on a vertical or horizontal column. This column is optically scanned over the screen once per image frame. As this system scans at the frame rate instead of the line rate, resulting in a reduction of three orders of magnitude, it has a more reliable optical scanning. At the same time the production of thousands of pixels is avoided. This is a cheaper system as well, because the expensive polygon scanner can be replaced by a cheap galvanometer-scanner. The idea behind this system was developed at Silicon Light Machines. Afterwards the rights were sold to Sony, where this system has been developed further.

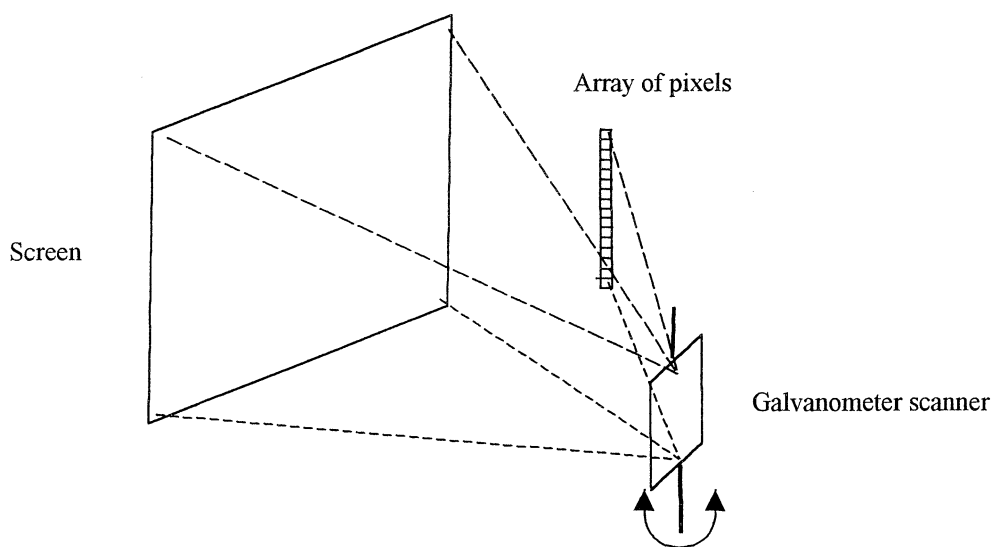


**Figure 2.10** The Scanned Linear Architecture.

## 2.7 Conclusion

To conclude the comparison of these different projector techniques, the plan for this project was to build a scanning system.

The first step was to construct a projector, which draws vector graphics. This means that the laser beam is not scanned over the whole screen, but instead only draws the contours of figures. This system is simpler because it is sufficient to use two “slow” and



cheap galvanometer scanners. However, some components will be the same for these systems and can be used for both set-ups.

After having understood how the different components in a vector graphics system work, the next step could be to replace the horizontal scanner by a fast spinning polygon mirror.

### 3. The Set-up

#### 3.1 The Components

The first set-up, see Figure 3.1, consisted of the following components: a laser, two galvanometer mirrors (scanners), two servo cards, a screen, a power supply and a function generator.

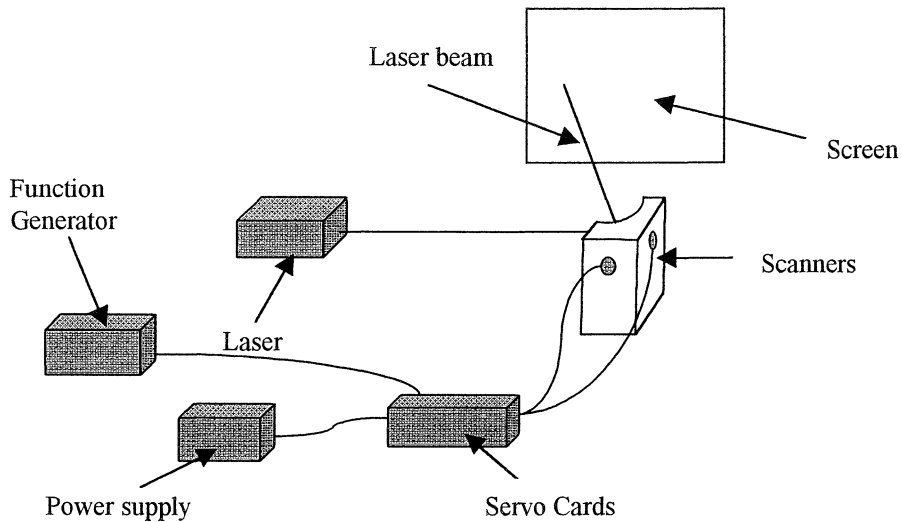


**Figure 3.1** The Set-up.

##### 3.1.1 The Laser

The laser used in my set-up is a Coherent COMPASS 315M-20. COMPASS (Compact Solid State) is a family of small, air-cooled, self-contained diode pumped Nd:YAG lasers. It is a Miniature CW laser which utilises an intra-cavity frequency-doubling crystal to convert IR emission to the green wavelength. It operates at 532 nm and its output power is 20 mW. As the human eye is very sensitive to green light, see Figure 3.2, the output power need not be higher.

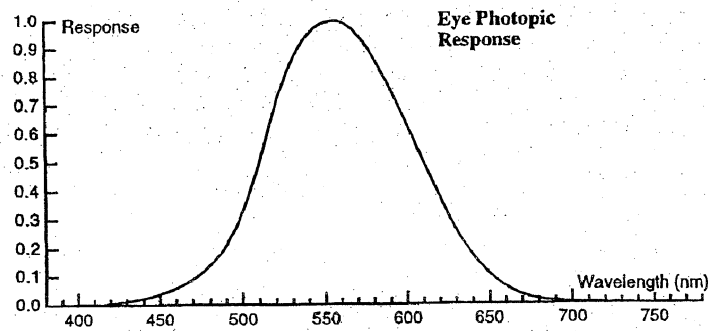


Figure 3.2 The response of the human eye.<sup>1</sup>

### 3.1.2 The Scanners and Servo Cards

The scanners and cards are parts of the 6800/CB6588 Mirror Positioning System by Cambridge Technology, Inc. The scanner has a fused silica mirror with a broadband hard dielectric coating.

The scanner is a moving-magnet actuator, which means that the rotor is a magnet. The rotor is situated inside a coil. When a current passes through the coil, a torque, which is proportional to the current, is created. Thus by changing the coil's current, the position of the scanners can be controlled. High torques can be created almost instantly because the electrical inductance is low and no saturation limit exists. However two practical factors limit the amount of the torque. The first one is the mechanical failure of the rotor assembly. The second is the maximum heat that the coil can conduct away without overheating the magnet. Nevertheless high performance can be achieved because both these factors are very high.

The accurate mirror positioning of this system can be achieved by an optical sensor, which detects the angular position of the shaft. An LED (Light Emitting Diode) shines on two photodiodes, which generate currents. A vane is attached to the rotor and casts shadows on the photodiodes. Depending on the position of the rotor the photodiodes detect different intensities of light. This causes the current from each to change correspondingly. These currents are converted to a voltage that is proportional to the rotor's angular position. By feeding back this voltage to the driver electronics, the signals needed, to get the rotor to the wanted position, can easily be determined.

When the scanners and the cards are used at high amplitude and high frequency for a longer period, they become warm. The scanners can be damaged if they get warmer than 50°C and the cards should not become warmer than 100°C. In order to avoid this, the scanners are arranged in an aluminium mount, which is attached to two heatsinks. The servo cards are bolted into an aluminium box. Thus all components have the possibility to lead away heat and none of them should become too hot.

Each scanner has to be connected to its servo card. The servo cards are identical but they are tuned to their respective scanner's mirror. As long as the mirrors' inertia do not change the system is ready to use. In case one mirror's inertia changes it is possible to retune the servo cards. The cards' main task is to convert the input signal they get from a computer or wave generator to an output signal, which is sent to the scanners, so that the mirror reaches the intended position. By comparing the input signal with the fed back signal from the photodiodes, an error signal is created. The aim is to minimise the error signal, which leads to the adjustment of the rotor's position.

### 3.1.3 The Power Supply and the Function Generator

The servo cards have to be supplied with power and moreover they need input signals, for example from a function generator. The scanners work optimal if the cards are supplied with  $\pm 28$  V. Thus this configuration is chosen. The constraints for the input signal are that the frequency should be less than 600 Hz and the amplitude should be varied between 1 V to 20 V peak to peak. If the amplitude, however, is increased above the  $\pm 10.6$  V limit, the over-position limiter on the servo cards starts to function and the signal is clipped. An over-heat limiter exists as well. This limiter will attenuate the input signal, if the scanner is operated at amplitudes and frequencies so that the power dissipated in the scanner approaches 10W.

## 3.2 The First Experiments

After having heatsinked the components properly and being sure that all the connections were correct, both the x and y scanners were tested on their own. First only the x-scanner and its card were used. When the laser was adjusted so that its beam hit the scanner in the middle of its mirror, the laser spot on the screen drew a horizontal line. Afterwards the y-scanner was tested on its own, which resulted in a vertical line on the screen. Increasing the amplitude of the input signal, which was used to control the scanners, increased the length of the line. When the input signal had a rather low frequency, it was possible to follow the laser spot with the eye. Increasing the frequency resulted in a flickering line, but at around 60 Hz the line was stable.

Depending on the waveform the lines were different as well. If a triangle wave was used, the line was very regular. If on the other hand a sine wave was used, the endpoints of the line became a bit brighter than the line connecting the points. Another possibility was a square wave, which resulted in a hardly visible line, but very bright endpoints. Considering the time interval the laser spot spent on each point on the screen, due to the chosen waveform, this behaviour was of course expected.

Having understood how each scanner was working, both scanners were used at the same time. In the beginning they were connected to the same input signal, thus the picture drawn was a line inclined  $45^\circ$ .

### 3.3 Improvements

The next step was to try drawing more “advanced” figures, such as squares, circles and any other figure, which consists of lines and circles. Moreover it should in the end be possible to write single letters and whole words.

In order to draw more complicated pictures, some improvements in the set-up had to be done, see Figure 3.3. The function generator had to be replaced by a computer, which worked in combination with a DAC board. Moreover an intensity modulator had to be included.

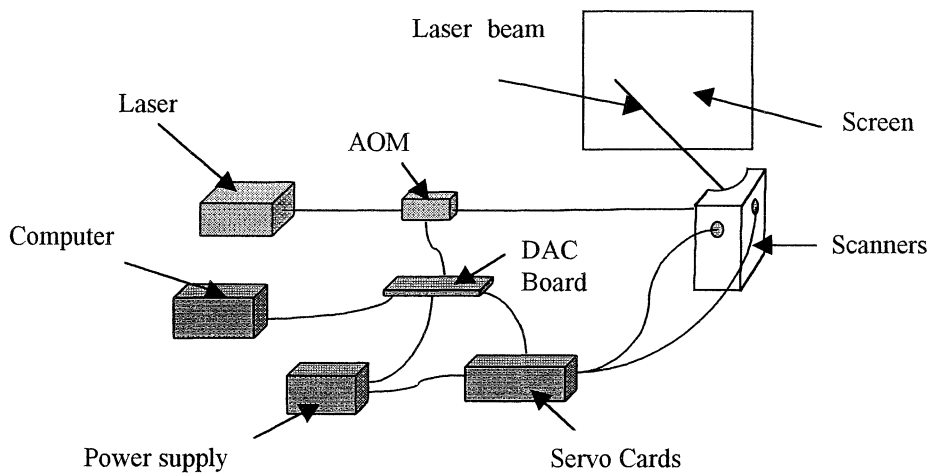


Figure 3.3 The modified set-up.

#### 3.3.1 The DAC Board

A special DAC board was needed, now that the computer replaced the function generator. This board was the link between the computer and the servo cards, which converted the computer's output signal to an appropriate input signal for the servo cards.

This board made it easier to control the scanners and let them draw more irregular figures, which not only consisted of periodic waves. The board itself had to be connected to a  $\pm 18$  V power supply and naturally to the scanners' servo cards. Moreover, data from the computer had to be transferred to the board in order to control the input signal to the scanners. The board consists of a flash card, which makes it possible to store data for an up to 5 minutes long laser show. However, the board can also be used without the flash card so that the scanners immediately respond to the data sent by the computer. Unfortunately this slowed down the process and the picture on the screen was not as regular as when the flash card was used.

### 3.3.2 The Software

The computer program responsible for sending data to the board is written in Delphi 5. This language is mostly using Pascal syntax, however it is object oriented. Several objects were used to implement a user-friendly interface. The first form used, which can be seen in Figure 3.4, consists of several different fields where the user determines what the figure to be drawn should look like. Several different waves can be chosen and superimposed for the x-, y- and z-axes. The choice stands between sine, cosine, triangle wave and nothing at all. Also the amplitude, the period and the phase can be chosen. For later use even the "concentration" for the different colours can be adjusted, in order to make it possible to display more colours than just the three colours the laser have. Besides the amplitudes, even here different phases and periods can be chosen.

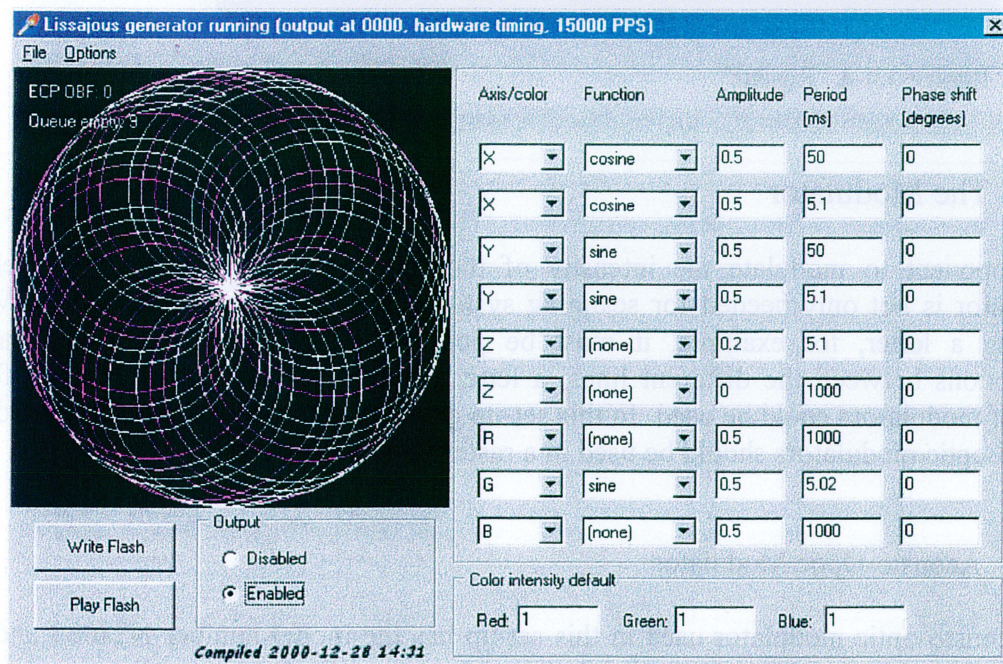


Figure 3.4 User Interface.

If the "Enabled" button is activated, the computer sends its data to the DAC board and the scanners draw the figure shown in the user interface. Finally, if the "Write Flash" button is pressed, the data is still sent to the DAC board, but not to the scanners. Instead it is saved on the flash card. After having saved enough information, it can be retrieved from the card by using the "Play Flash" button and the scanners start drawing the figure, see Figure 3.5.

Afterwards the program was expanded so that also letters and whole words in general could be displayed. The final aim is to let the user determine the displayed text by simply typing the wanted letters on the keyboard.

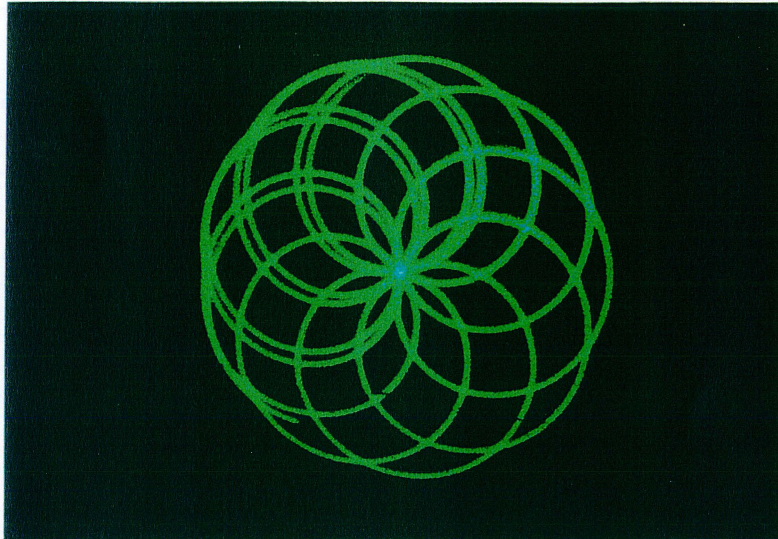


Figure 3.4 A “Rosette”

### 3.3.3 The Modulator

A component to modulate the intensity of the laser beam was needed, as well. A modulator is not only needed for scanning systems but also for vector graphics. When drawing a letter, for example, it must be possible to blank the laser, so that no connections between the different lines, a letter consists of, are visible. Two different sorts of modulators could be used. In this set-up an acousto-optic modulator is tested, but electro-optic modulators should be used in a raster scanned systems.

#### 3.3.3.1 Acousto-Optic Modulator

The acousto-optic modulator used in this set-up has the model number N23080 and is a product from Newport Electro Optics Systems, Inc. Acousto-Optic modulators consist of a crystal, which is connected to a piezoelectric transducer. By sending radio frequency signals to the transducer, acoustic waves are generated in the crystal, see Figure 3.6. These waves result in a periodic wave pattern in the crystal, consisting of compressed and rarefacted areas. As the index of refraction depends on the density, the index of refraction changes periodically as well. The incident light is diffracted by this structure in the same way as a grating diffracts light.

The amount of diffracted light depends on the amplitude of the acoustic waves in the crystal. Thus by modulating the amplitude of the radio frequency signal it is possible to modulate the intensity of the diffracted laser beam.

The AOM has to be properly adjusted in order to work correctly. The intensity of the laser beam is not attenuated much by the AOM, as its absorption is low.

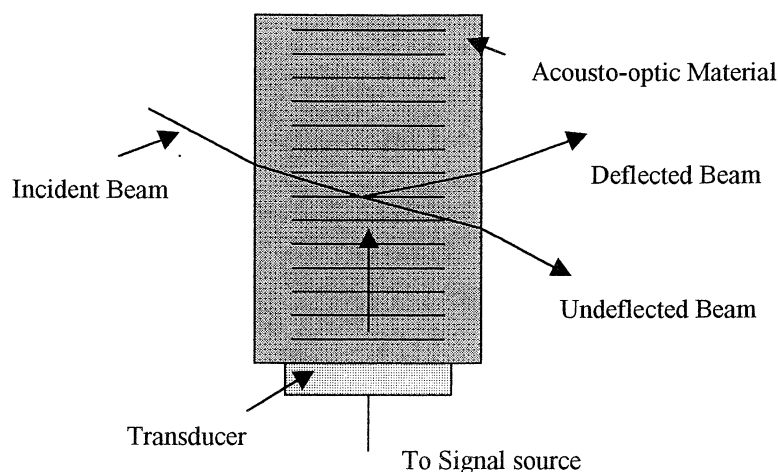


**Figure 3.6** The Acousto-optic Modulator.

The first and higher order maxima of course only appear if the AOM is placed in the beam and is turned on because otherwise there are no acoustic waves and thus no grating, which can diffract. One of the first order maxima was used to draw the pictures, as first orders maxima are the most intense. All the other orders were filtered away, simply by only letting this first order maximum hit the scanner. Thus it was possible to totally turn off the laser spot on the screen by turning the amplitude of the radio frequency signal to almost zero.

### 3.3.3.2 Electro-Optic Modulator

Electro-optic modulators can also be used for intensity modulation. They make use of the electro-optic effect that exists in non-centro-symmetric crystals. Electro-optic modulators will be treated in detail in chapters 4-6.

### 3.3.4 Using the AOM for Blanking

To be able to write letters, the AOM had to be connected to the DAC board as well. While drawing circles and other closed figures the AOM was not needed because the laser beam never needed to be blocked. Drawing letters on the other hand often involves moving the laser beam from one point to another point, while the line connecting these points should not be visible. Thus the board needed to send signals to the AOM in order to turn it on and off at the correct co-ordinates and moments. This means that the program had to be altered. Besides of calculating all the points different letters consist of, it also had to send a special signal when it was time to block the laser beam.



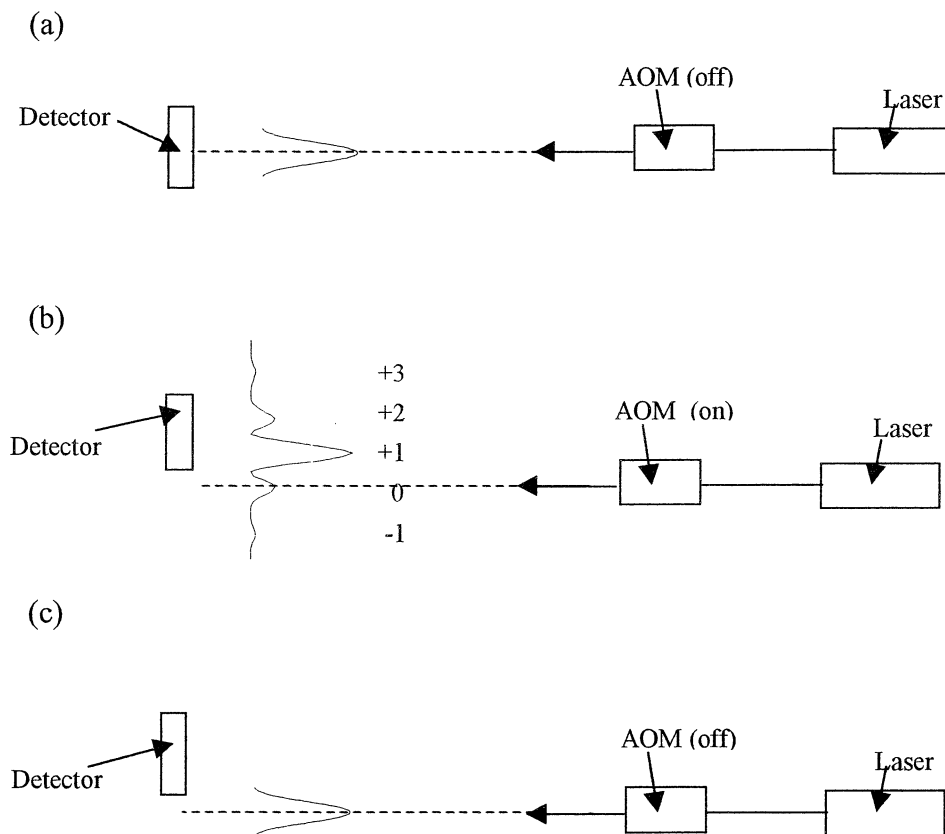


**Figure 3.7** (a) The AOM is turned off, detector registers 0th order maximum. (b) AOM is turned on, detector registers 1st and 2nd positive maxima. (c) AOM is turned off, detector still at the position from (b).

In the set-up the AOM was placed directly behind the laser. When the AOM was turned off only one laser beam (the undeflected) left it. The intensity detected by a photodetector was then 23.8 mW, see Figure 3.7 (a). If the AOM on the other hand was turned on, a diffraction pattern consisting of 5 maxima appeared. If the photodetector was adjusted so that it only measured the intensity of the first and second positive maxima the result was 22.2 mW, see Figure 3.7 (b). Leaving the detector in its position and turning off the AOM, only the central maximum remained. But as this maximum was not focused onto the detector, the detector only registered an intensity of 27  $\mu$ W, see Figure 3.7 (c). These values show that the AOM is rather efficient, as it is possible to deflect 22.2 mW out of the possible 23.8 mW into the first and second positive maxima, which is 93%. Moreover the contrast ratio, which is the percentage of the laser intensity passing through the AOM although it is turned off, is approximately 0.1%.

Finally, as the laser beam now could be blocked it was possible to write text and to draw complicated pictures as can be seen in Figure 3.8.

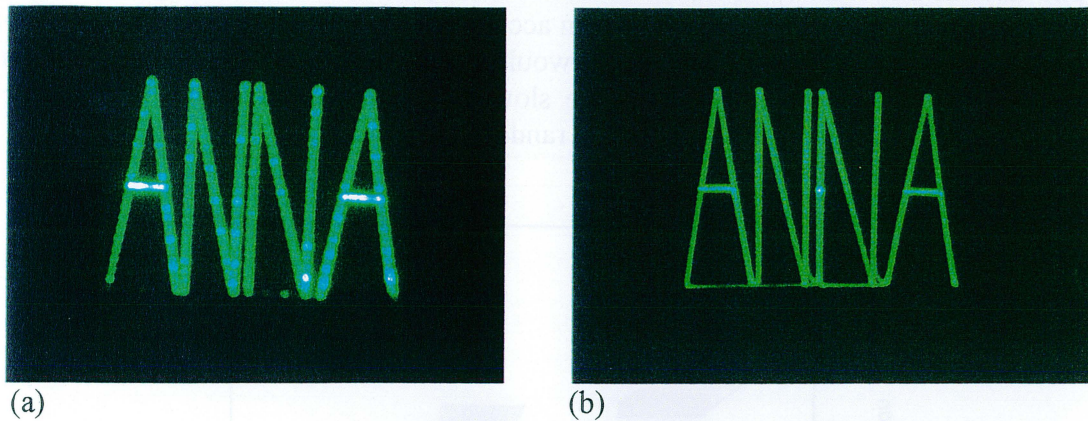


**Figure 3.8** The Display. (a) Data is not stored on the Flash Card. (b) Data is stored on the Flash Card

However some problems occurred when letters were drawn. When the data was not saved on the Flash Card, but immediately transferred to the scanners, the picture was flickering, due to the limited speed at which the points can be supplied by the computer. Moreover the individual points, each letter consists of, were visible, as the laser beam paused on these co-ordinates because of the low point supply rate.

On the other hand, when the data was stored on the Flash Card, the picture was stable and more regular. However certain irregularities occurred because drawing letters involves quick changes of directions for the scanners. Moreover the AOM did not seem to work as effectively at high rates and in combination with the Flash Card, which resulted in certain lines being visible which should have been invisible.

### 3.4 Possibilities to Develop the Raster-Scanned Projection System

From the beginning the plan was not to stop after having achieved a working vector graphics system, but to try to build a scanning full-picture projector.

However, in order to build a raster scanned system, another sort of deflectors than the galvanometer scanners is needed. Drawing PAL pictures with the resolution  $720 \times 576$  and a picture scan rate of 50 Hz, requires that 28800 horizontal lines are scanned per second. This is impossible with the galvanometer scanners, which only work at frequencies below 600 Hz. In general three different types of deflectors exist: mechanical, acousto-optic and electro-optic deflectors. These types differ in terms of their resolution and their access time, which are the two main factors determining the performance of a deflector.

Light-beam deflection is measured in terms of resolvable spots, rather than in terms of the absolute angle of deflection. One resolvable spot means that the beam is deflected by an angle equal to its own angular spread. The access time is the random-access time to acquire one specific spot or resolution element. Figure 3.9 indicates that mechanical methods give the largest number of resolvable spots, but are slowest, whereas electro-

optic devices are fastest, but have the smallest number of resolvable spots. The figure characterises the speed in terms of random access time to reach any desired spot. Another possible method of characterising speed would be the spot scan rate during a sequential scan. Again the mechanical systems are slowest and the electro-optic fastest, but the difference is less pronounced than for the random-access time.<sup>5</sup>

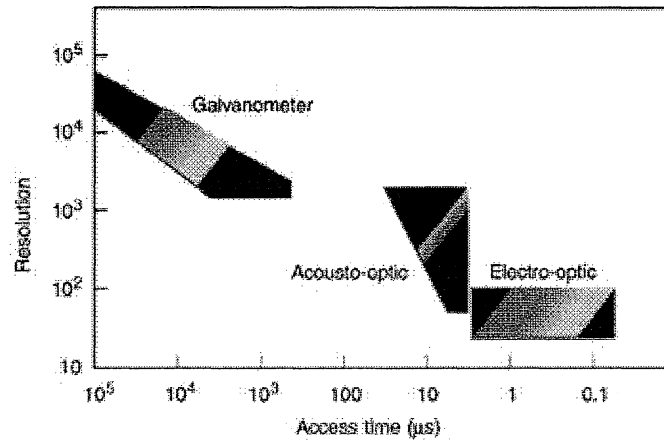


**Figure 3.9** Possible resolution as a function of the access time for three different sorts of deflectors.<sup>5</sup>

None of the three alternatives mentioned above fulfil the criteria of both high resolution and low access time. However an alternative mechanical scanner to the galvanometer scanner exists, the polygon mirror. This mirror could replace the galvanometer scanner, which is responsible for the x-axis. By using a fast spinning polygon much more lines can be drawn per second than with a galvanometer scanner. This is exactly what was needed for a scanning system. Unfortunately such polygon scanners are very expensive – too expensive for the available budget – and it was impossible to borrow one.

## 4 The Electro-Optic Modulator – Theory

An alternative to the AOM is an electro-optic modulator (EOM). Electro-optic modulators are faster than acousto-optic modulators and can modulate at rates as high as several GHz. An EOM consists of an anisotropic crystal. Depending on the voltage applied to this crystal the state of polarisation of a wave passing through the crystal can be changed in a desired manner.

### 4.1 Anisotropic Crystals

When an electromagnetic wave is incident on an anisotropic crystal, waves propagate with different phase velocities depending on the direction of polarisation. An uniaxial crystal for example is birefringent. This means that the electric susceptibility and permeability coefficients of one axis differ from the coefficients of the other two axes. Thus the crystal has two indices of refraction, resulting in two different phase velocities. The conventional notation is that  $n_x = n_y \neq n_z$ . For a wave propagating along the z-axis, the x- and y-components will see the same index of refraction  $n_0$ . As the crystal behaves optically isotropic in this direction, the z-axis is called the optical axis. A wave propagating along the x-axis however consists of components, which experience different indices of refraction. The y-component, which is called the ordinary ray, will travel with a phase velocity according to  $n_x = n_y = n_0$ , whereas the extraordinary ray, which is parallel to the z-axis, will have a phase velocity according to  $n_z = n_e$ .

Consider a wave propagating along the x direction which is linearly polarised having two equal components along y and z. As these components travel with different velocities through the crystal they get out of phase and the wave becomes elliptically polarised.

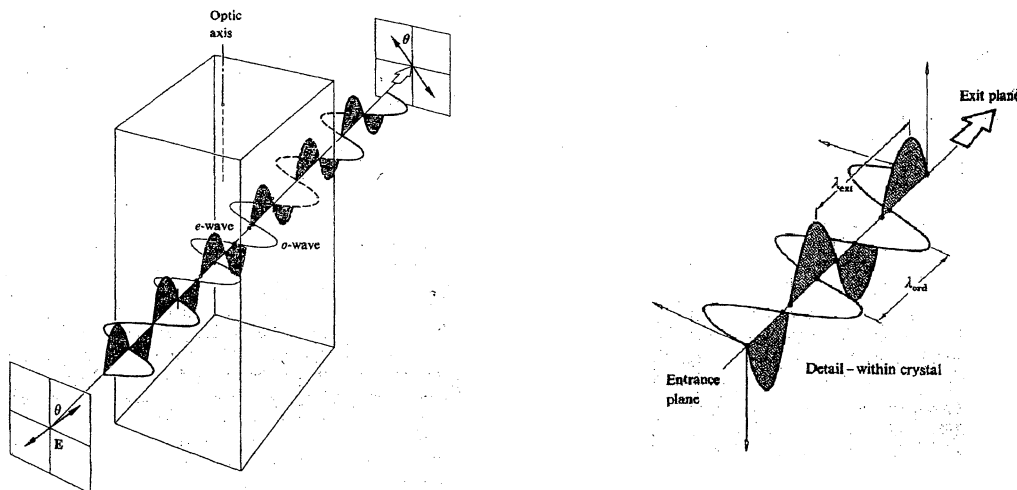


Figure 4.1 Direction of polarisation is rotated 90° by a crystal.<sup>7</sup>

Depending on the length of the crystal the wave's state of polarisation will vary after having passed the crystal. If the phase difference after the crystal is  $\pi$ , the wave will be linearly polarised but  $90^\circ$  rotated in relation to the incoming wave, see Figure 4.1.

The crystals used in this experiment are biaxial, which means that  $n_x \neq n_y \neq n_z \neq n_x$ . In this case no axis can be denoted ordinary or extraordinary. In the experiment the light will travel along the x-axis and will have two components, one parallel to the y-axis and the other one parallel to the z-axis. Thus this case is comparable to the uniaxial case because the fact that  $n_x \neq n_y$  does not have any influence on the phase shift between the y- and the z-component, which is the only interesting relationship for electro-optic modulators.

## 4.2 The $\text{KTiOPO}_4$ Isomorphs

The crystals used in this project are members of the  $\text{KTiOPO}_4$  (KTP) family. The elements of this family are characterised by the formula  $\text{MTiOXO}_4$ , where M can be K, Rb or Cs and X either P or As. The KTP family members are non-centro-symmetric crystalline materials and are used in various non-linear-optical applications. They are orthorhombic and belong to the acentric group  $\text{mm}2$ . Their structure is characterised by chains of  $\text{TiO}_6$  octahedra, which are linked at two corners and separated by  $\text{XO}_4$  tetrahedra. The M ion is weakly bonded to the Ti octahedra and the X tetrahedra. See Figure 4.2.

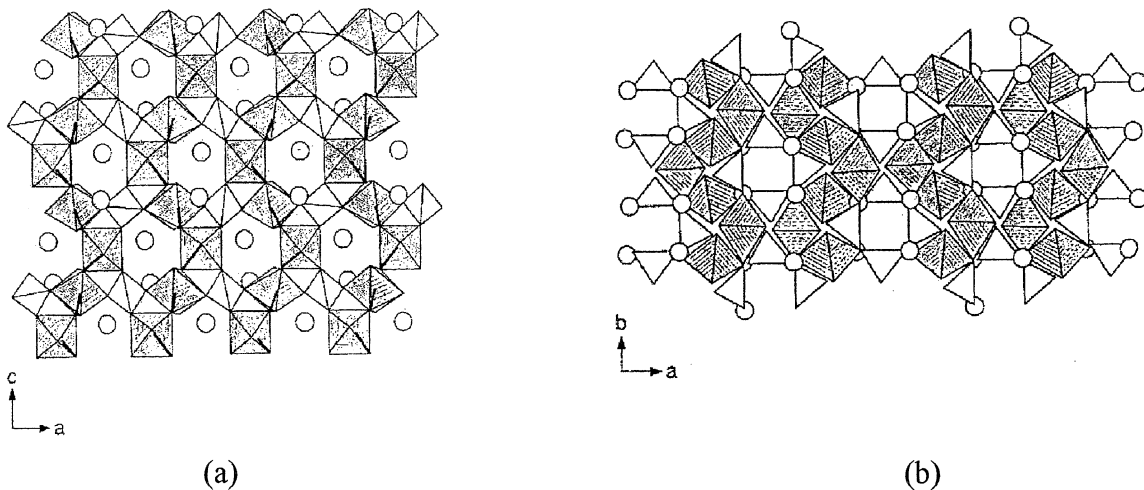


**Figure 4.2** Structure of KTP: (a) a-c (x-z) projection, (b) a-b (x-y) projection. Shaded elements are the  $\text{TiO}_6$  octahedra, open elements are the  $\text{PO}_4$  tetrahedra and open circles are the K. The short Ti-O bonds are shown as bold lines.<sup>8</sup>

Channels exist in the crystal lattice along the z-axis whereby M ions can move through a vacancy mechanism with a diffusion constant several orders of magnitude higher than in the x-y plane.

When KTP isomorphs are grown the crystal looks as in Figure 4.3. The samples, which are examined, are KTP,  $\text{KTiOAsO}_4$  (KTA),  $\text{RbTiOPO}_4$  (RTP) and  $\text{RbTiOAsO}_4$  (RTA).

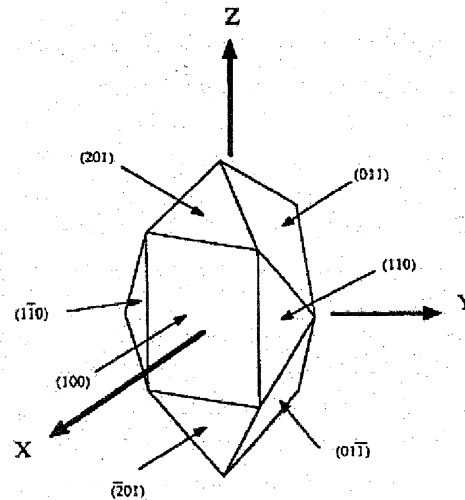


Figure 4.3 KTP crystal morphology.<sup>6</sup>

### 4.3 The Electro-Optic Effect

Depending on the length of the anisotropic crystal a wave's state of polarisation will vary after having passed the crystal. Fortunately, there is another way to control the state of polarisation of a wave incident on a crystal, other than changing the length of the crystal. By applying an electric field to a crystal, the indices of refraction for the axes are changed. In crystals, which do not possess inversion symmetry, the linear electro-optic effect - the Pockels effect - causes small changes of the index of refraction, which are proportional to the applied field. This is the effect used in EOMs. Even a non-linear, quadratic electro-optic effect, which is called Kerr effect, exists, but for moderate electric fields this effect is smaller than the linear effect and will be neglected.

Every material has a characteristic electro-optic tensor, which for this purpose can be reduced to a  $3 \times 6$ -element matrix. The form, but not the magnitude, of the matrix can be derived from symmetry considerations. In a crystal with inversion symmetry all the coefficients are zero, whereas in a triclinic crystal, which has no symmetries at all, all coefficients are nonzero and different. Biaxial material, however, have some symmetries and they have only a few nonzero elements. The matrices for KTP, RTP, KTA and RTA can be found in literature, see Table 4.1.

KTP	RTP	KTA	RTA
$\begin{pmatrix} 0 & 0 & 9.5 \\ 0 & 0 & 15.7 \\ 0 & 0 & 36.3 \\ 0 & 9.3 & 0 \\ 7.3 & 0 & 0 \\ 0 & 0 & 0 \end{pmatrix}$	$\begin{pmatrix} 0 & 0 & 10.9 \\ 0 & 0 & 15 \\ 0 & 0 & 33 \\ 0 & * & 0 \\ * & 0 & 0 \\ 0 & 0 & 0 \end{pmatrix}$	$\begin{pmatrix} 0 & 0 & 11.5 \\ 0 & 0 & 15.4 \\ 0 & 0 & 37.5 \\ 0 & * & 0 \\ * & 0 & 0 \\ 0 & 0 & 0 \end{pmatrix}$	$\begin{pmatrix} 0 & 0 & 13.5 \\ 0 & 0 & 17.5 \\ 0 & 0 & 40.5 \\ 0 & * & 0 \\ * & 0 & 0 \\ 0 & 0 & 0 \end{pmatrix}$

**Table 4.1** The electro-optic coefficients for KTP isomorphs. The elements marked by an asterisk have not been measured.<sup>6</sup>

The index of refraction for crystals depends upon the incident wavelength and can be calculated by using the Sellmeier equation

$$(4.1) \quad n_i^2 = A_i + \frac{B_i}{1 - \left(\frac{C_i}{\lambda}\right)^2} - D_i \lambda^2, \text{ where } i = x, y, z. \text{ }^6$$

The wavelength  $\lambda$  has to be in  $\mu m$  and the different sets of Sellmeier coefficients can be found in literature. For KTP isomorphs see Table 5.1 on page 33.

The equations describing the change of the indices of refraction, when an electric field is applied to a crystal, depend on the structure of the material. Moreover the equations also depend on which axis the voltage is applied to. The KTP family is a member of the orthorhombic mm2 crystals and the changes of the indices of refraction for these materials, if the voltage is applied along the z-axis, are equal to:

$$(4.2) \quad \Delta n_y = \frac{1}{2} r_{23} n_y^3 E_z^e, \text{ for the y-component and}$$

$$(4.3) \quad \Delta n_z = \frac{1}{2} r_{33} n_z^3 E_z^e, \text{ for the z-component.}$$

$r_{23}$  and  $r_{33}$  are the appropriate crystal's electro-optic coefficients and  $E_z^e$  is the electric field applied to the crystal along the z-axis.

Thus the changes of the index of refraction are proportional to the applied voltage, as  $E = \frac{V}{d}$ , where  $V$  is the applied voltage and  $d$  the crystal's thickness. Moreover it is evident that the only elements of the 3x6 electro-optic matrix, which are important when the crystal used is a member of the KTP family and the electric field is applied along the z-axis, are  $r_{23}$  and  $r_{33}$ .

The total phase shift for the component, which is parallel to the y-axis, after having travelled a distance  $x$  inside the crystal, is

$$(4.4) \quad \varphi_y = k_0 n_y x = k_0 x \left( n_y - \frac{1}{2} n_y^3 r_{23} \frac{V_0}{d} \right)$$

where  $V_0$  is the applied voltage,  $d$  the crystal's thickness and  $k_0$  the incident light's wavevector in vacuum.

And for the component, which is parallel to the z-axis, the phase shift is

$$(4.5) \quad \varphi_z = k_0 n_z x = k_0 x \left( n_z - \frac{1}{2} n_z^3 r_{33} \frac{V_0}{d} \right)$$

These expressions lead to the following equation for the phase difference between the two components after having passed a crystal of length  $l$

$$(4.6) \quad \Delta\varphi = \varphi_y - \varphi_z = k_0 (n_y - n_z) l + \frac{1}{2} k_0 n_z^3 r_{33} \frac{V_0}{d} l - \frac{1}{2} k_0 n_y^3 r_{23} \frac{V_0}{d} l$$

Thus, the field induced phase retardation is

$$(4.7) \quad \Gamma = \frac{\pi}{\lambda} n_z^3 r_{33} \frac{V_0}{d} l - \frac{\pi}{\lambda} n_y^3 r_{23} \frac{V_0}{d} l.$$

This can be written as

$$(4.8) \quad \Gamma = \frac{\pi}{\lambda} n_z^3 r_c \frac{l}{d} V, \text{ where}$$

$$(4.9) \quad r_c = r_{33} - \left( \frac{n_y}{n_z} \right)^3 r_{23}.$$

The voltage needed to obtain a phase retardation of  $\Gamma = \pi$  is called half-wave voltage and denoted by  $V_\pi$ .

Using Equation (4.8) this voltage is found to be

$$(4.10) \quad V_\pi = \frac{\lambda d}{n_z^3 r_c l}.$$

Thus, the longer and the thinner the used crystal is, the lower can the applied voltage be, in order to rotate the direction of polarisation  $90^\circ$ . Another variable, which can be adjusted in order to minimise the half-wave voltage, is  $r_c$ . In general, voltage is applied to the axis, which maximises  $\Gamma$ , which in KTP isomorphs happens to be the z-axis. However, if the light had travelled along the y-axis instead of the x-axis, the phase difference had been even higher, as  $n_x$  is smaller than  $n_y$  and  $r_{13}$  is smaller than  $r_{23}$ , resulting in an increased value for  $r_c$ . As the crystals used in this experiment were



polished so that the light had to travel along the x-axis, the half-wave voltage could no be further decreased.

The calculations made above are for a transverse modulator, where the electric field is applied normal to the direction of light propagation. Another type of modulator, where the electric field is applied along the direction of propagation, exists as well, the longitudinal modulator. The main disadvantage for this modulator is that the field electrodes interfere with the optical beam.

However, the choice of using transversal or longitudinal modulators depends on the structure of the crystal, e.g. the KTP isomorphs cannot be used in longitudinal modulators. If voltage is applied along the same direction as the light is travelling, no phase shift due to the applied voltage will occur, as the electro-optic coefficients representing these phase shifts,  $r_{41}$ ,  $r_{52}$  and  $r_{63}$ , are zero.

## 4.4 The Principle for an Electro-Optic Modulator

A transverse electro-optic modulator consists of two polarisers, a quarter-wave plate and an electro-optic crystal, which is oriented so that the voltage is applied normal to the light's direction of propagation.

The first polariser is adjusted with its direction of polarisation at  $45^\circ$  to the vertical axis. Thus after having passed this polariser, the wave is linearly polarised and consists of two perpendicular components. The component, which is parallel to the y-axis and the component, which is parallel to the z-axis, both have the same size. These components travel with different velocities, as the indices of refraction are different. According to Equation (4.8) the field induced phase retardation is proportional to the applied voltage. If the applied voltage is  $V_\pi$ , the direction of polarisation is rotated  $90^\circ$ . However the phase difference due to the birefringence of the material has to be taken into consideration as well. This value is for a 10 mm long crystal of the order 100 000 radians. Thus this retardation is very large in comparison to the field induced phase retardation. In order to eliminate the constant contribution of the phase shift a quarter-wave plate is situated behind the crystal. Behind this plate another polariser is situated. If the polarisation of the analyser and the quarter-wave plate are correctly adjusted the intensity of the light, after having passed the analyser, can be controlled by the applied voltage.

If no voltage is applied to the crystal, the polarisation of the light after having passed the crystal and the quarter-wave plate is orthogonal to the analyser's polarisation. Thus no light will pass through the analyser and the laser beam is blocked, see Figure 4.4.

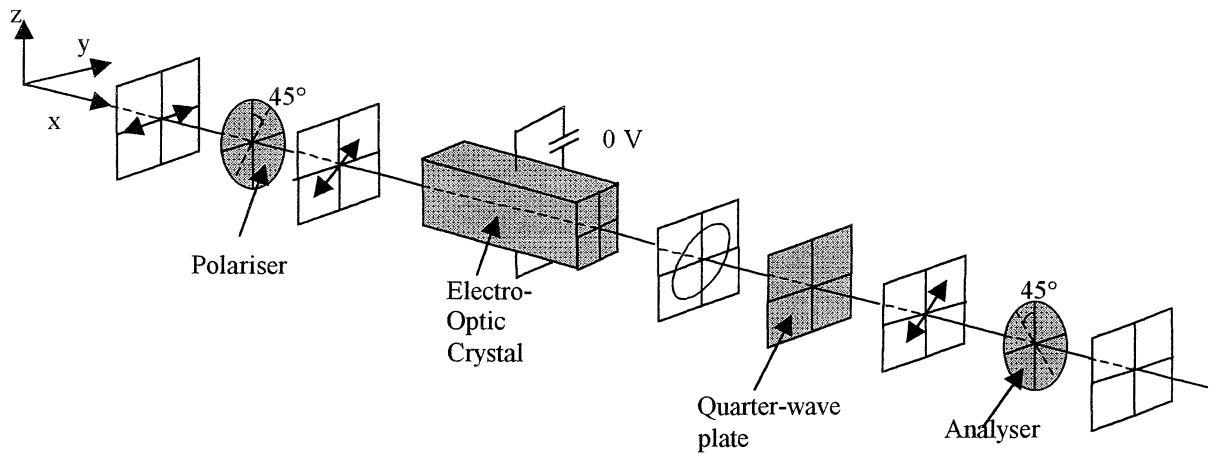


**Figure 4.4** Blocking the laser beam. Applied voltage is 0 V.

If the applied voltage is  $V_{\pi}$  on the other hand, the polarisation after having passed the crystal and the quarter-wave plate will be parallel to the analyser's polarisation. This means that the intensity is the highest possible, taking into consideration that the laser beam is attenuated by the different components, see Figure 4.5.

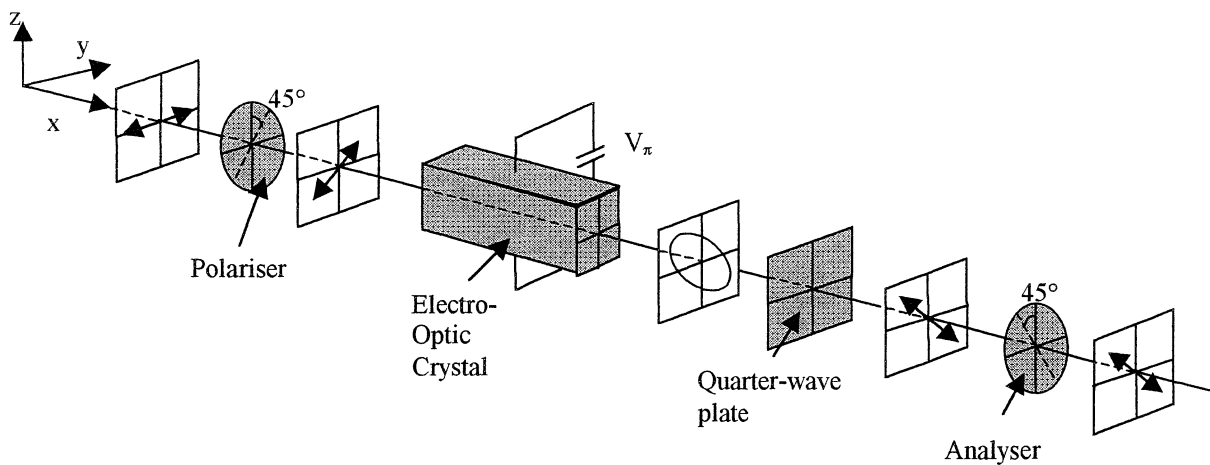


**Figure 4.5** Letting the laser light pass. Applied voltage is  $V_{\pi}$ .

In general, the intensity of the light after having passed the modulator is

$$(4.11) \quad I_{out} = I_{in} \alpha \sin^2\left(\frac{\Gamma}{2}\right) = I_{in} \alpha \sin^2\left[\left(\frac{\pi}{2}\right) \frac{V}{V_{\pi}}\right]$$

where  $I_{in}$  is the incident intensity,  $I_{out}$  is the output intensity and  $\alpha$  is a constant representing the attenuation due to reflection and absorption in the two polarisers, the electro-optic crystal and the quarter-wave plate.

Another set-up, where less light is wasted before reaching the crystal, is possible. Instead of using a polariser to receive two perpendicular components of equal size, one parallel to the y-axis and the other one parallel to the z-axis, the crystal can be rotated  $45^\circ$ . This will result in two perpendicular components, without using the first polariser, which decreases the amplitude of the incoming light by a factor of  $\frac{1}{\sqrt{2}}$ .

## 5 The First Electro-Optic Modulator – Calculation, Construction and Testing

Most modulators are built for the IR region. For these wavelengths the most common electro-optic crystals are LN ( $\text{LiNbO}_3$ ) and LT ( $\text{LiTaO}_3$ ). Unfortunately these materials are susceptible to so-called photorefractive damage, when used with visible light, which makes them less useful in this wavelength regime. In the photorefractive process electrons are excited from defects in the lattice, mostly through ionisation of  $\text{Fe}^{2+}$ . All the excited free electrons are drifting in the static electric field that these crystals have, and become trapped outside the illuminated region. An electric field is now set up between the trapped electrons and the ionised defects ( $\text{Fe}^{3+}$ ). This field is changing the refractive index of the illuminated region through the electro-optic effect and finally leads to distortion of the transmitted beam.

In KTP isomorphs, on the other hand, the conductivity is higher than in LN and LT, i.e. that the trapped electrons can be neutralised by the K or Rb ions, which can move in the channels along the z-axis. Thus, this modulator will be using a KTP family member as the electro-optic crystal in the EOM.

### 5.1 Absorption Coefficient for the KTP Isomorphs

The task of the electro-optic crystal inside a modulator is naturally to modulate the incident light. However, material attenuates light so that the light's intensity is reduced due to absorption and reflection. The material used for modulators should therefore have low absorption coefficients, which has to be checked.

#### 5.1.1 How to Determine Absorption Coefficients

As stated in chapter 4.2 five different crystals belonging to the KTP family exist: KTP, KTA, RTP, RTA and CTA. Samples from the first four materials were available. First, a series of measurements were done in order to determine the absorption coefficients for the different samples. The absorption coefficients can vary due to impurities, which can enter the material during the different steps in the growth procedure.

When an electromagnetic wave is incident on a surface, some part of the wave is reflected back. Moreover the wave is attenuated when passing through material. Thus the intensity of the light after having passed a crystal will not be the same as it was before entering the crystal.

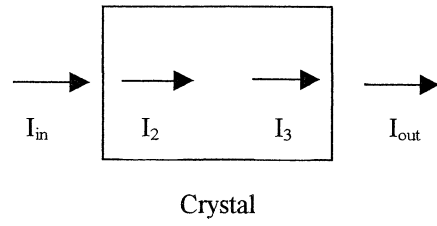


**Figure 5.1** The intensity of light passing through a crystal changes due to interfaces and due to absorption in the material.

The intensity transmitted through the first surface is

$$(5.1) \quad I_2 = TI_{in}.$$

T is the transmittance, which in case of normal incidence, is given by

$$(5.2) \quad T = \frac{4n_{air}n_{crystal}}{(n_{air} + n_{crystal})^2}, \quad n_{air} = 1.00029.$$

The transmittance values for the KTP family can be found in Table 5.2.

Inside the crystal the intensity decreases according to

$$(5.3) \quad I_3 = I_2 e^{-\alpha l}$$

where  $\alpha$  is the absorption coefficient and  $l$  the distance travelled within the crystal.

Finally, the part, which is transmitted through the second surface, is given by

$$(5.4) \quad I_{out} = TI_3$$

Combining these equations, results in the following relation between the input and the output intensities

$$(5.5) \quad I_{out} = T^2 e^{-\alpha l} I_{in}$$

The Sellmeier equation, which is used to determine the indices of refraction for certain materials at specific wavelengths, was stated in Equation (4.1). The Sellmeier coefficients  $A_i, B_i, C_i, D_i$  for the KTP family can be found in Table 5.1.

	KTP	RTP	KTA	RTA
<b>A<sub>x</sub></b>	2.11460	2.15559	2.11055	2.22681
<b>B<sub>x</sub></b>	0.89188	0.93307	1.03177	0.99616
<b>C<sub>x</sub></b>	0.20861	0.20994	0.21088	0.21423
<b>D<sub>x</sub></b>	0.01320	0.01652	0.01064	0.01369
<b>A<sub>y</sub></b>	2.15180	2.38494	2.38888	1.97756
<b>B<sub>y</sub></b>	0.87862	0.73603	0.77900	1.25726
<b>C<sub>y</sub></b>	0.21801	0.23891	0.23784	0.20448
<b>D<sub>y</sub></b>	0.01327	0.01583	0.01501	0.00865
<b>A<sub>z</sub></b>	2.31360	2.27723	2.34723	2.28779
<b>B<sub>z</sub></b>	1.00012	1.11030	1.10111	1.20629
<b>C<sub>z</sub></b>	0.23831	0.23454	0.24016	0.23484
<b>D<sub>z</sub></b>	0.01679	0.01995	0.01739	0.01583

**Table 5.1** Sellmeier coefficients for KTP isomorphs.<sup>6</sup>

In the experiment green light with the wavelength  $\lambda=0.532 \mu\text{m}$  was used. The indices of refraction calculated at this wavelength can be found in Table 5.2.

	KTP	RTP	KTA	RTA
<b>n<sub>x</sub></b>	1.77899	1.80446	1.82528	1.84713
<b>n<sub>y</sub></b>	1.78997	1.81726	1.83255	1.8575
<b>n<sub>z</sub></b>	1.8868	1.91043	1.93009	1.94462
<b>T</b>	0.905714	0.90223	0.89932	0.89717

**Table 5.2** The indices of refraction for the KTP isomorphs at  $\lambda=0.532 \mu\text{m}$ .

### 5.1.2 The Measurements Done for Determination of Absorption Coefficients

According to Equation (5.5) it is possible to determine each crystal's absorption coefficient by measuring the input and the output intensities and the crystal's length. Several crystals from each of the KTP isomorphs were available. Moreover several measurements were done for each sample, so that an average value was received.

Sample	RTP 16	RTP 17	RTP 18	RTP 19
$\alpha[\text{m}^{-1}]$	2.77	2.68	3.31	3.89

Table 5.3 Absorption coefficient for RTP crystals.

Sample	RTA 26	RTA 27	RTA 28	RTA 29
$\alpha[\text{m}^{-1}]$	3.49	2.70	1.87	2.04

Table 5.4 Absorption coefficient for RTA crystals.

Sample	KTA 3/58	KTA 4/59
$\alpha[\text{m}^{-1}]$	1.06	0.66

Table 5.6 Absorption coefficient for KTA crystals.

Sample	KTP 866
$\alpha[\text{m}^{-1}]$	1.34

Table 5.4 Absorption coefficient for a RTP crystal.

This experiment shows that these four members of the KTP family absorb an almost equally small part of the incoming light. On the other hand, the conductivity in both KTP and KTA are so high that an ionic current flows, when voltage is applied to the crystal and the material decomposes. Thus either RTA or RTP crystals have to be used as electro-optic crystals in modulators operating in the visible region. For us, almost no RTA was available, but some RTP “left-overs” were available, and hence RTP was used to construct a modulator.

## 5.2 Construction of the EOM

The central part of the EOM is of course the crystal, in this case RTP. The first step was thus to cut a crystal into the desired dimensions and polish it. As the applied voltage needed to rotate the direction of polarisation depends on the size of the crystal, the dimensions should be chosen in a way to minimise the voltage. The available crystals' dimensions were  $l = 10\text{ mm}$ ,  $d = 1\text{ mm}$ , which according to (4.10) gives acceptable values for the half-wave voltage.

In order to apply voltage to the crystal, along its z-axis, two contacts had to be made – one on the top and one on the bottom of the crystal as can be seen in Figure 5.3. The electric field in the crystal should be as uniform as possible. Thus the voltage must not be

applied at a single point. Therefore the whole top and the bottom surfaces of the crystal were covered by an electrically conducting silver-paste. The wires connected to the power generator were not soldered directly onto the crystal because the crystal should not be moved if the wires were accidentally pulled.

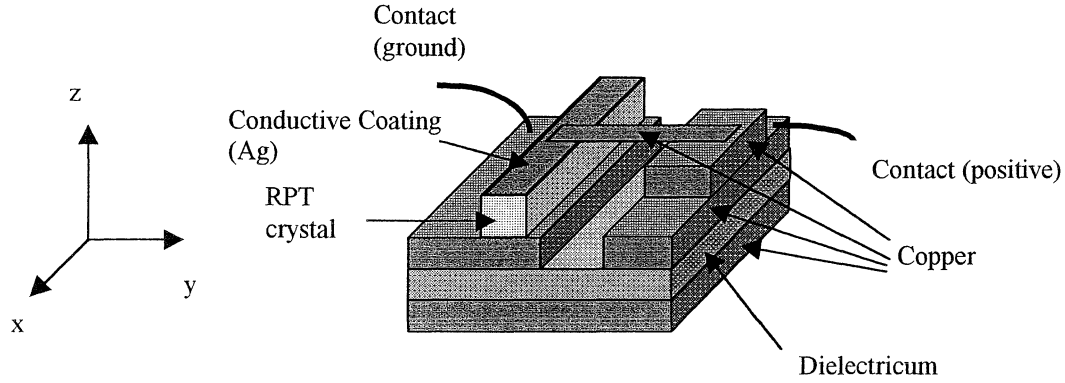


Figure 5.3 The electro-optic crystal and its contacts.

### 5.3 First experiments

Before starting the measurements it is possible to determine the half-wave voltage theoretically by using Equations (4.9) and (4.10). In the calculation the following data is used:

$$l = 10 \text{ mm}, d = 1 \text{ mm}, n_o = 1.81726, n_e = 1.91043, r_{23} = 15 \cdot 10^{-12} \frac{\text{m}}{\text{V}}, r_{33} = 33 \cdot 10^{-12} \frac{\text{m}}{\text{V}}$$

and  $\lambda = 532 \text{ nm}$ .<sup>6</sup>

This leads to the value  $r_c = 20 \cdot 10^{-12} \frac{\text{m}}{\text{V}}$ , which results in the half-wave voltage being  $V_\pi = 380 \text{ V}$ .

After knowing the theoretical half-wave voltage value, the practical was determined. Thus the crystal was placed between crossed polarisers, as shown in Figures 4.3 and 4.4. Voltage was applied to the crystal and was slowly scanned from 0 V to 550 V. The intensity of the light passing through the EOM was measured. The first measurement is shown in Figure 5.4. From the graph the half-wave voltage can be determined to approximately 400 V. This graph can be compared with the theoretical graph which is received when  $V_\pi = 400 \text{ V}$  is used in formula

$$(5.6) \quad I_{out} = I_{in} a \sin^2 \left( \frac{\pi V}{2 V_\pi} - b \right)$$

with appropriate constants a and b to make the maxima of both curves coincide.



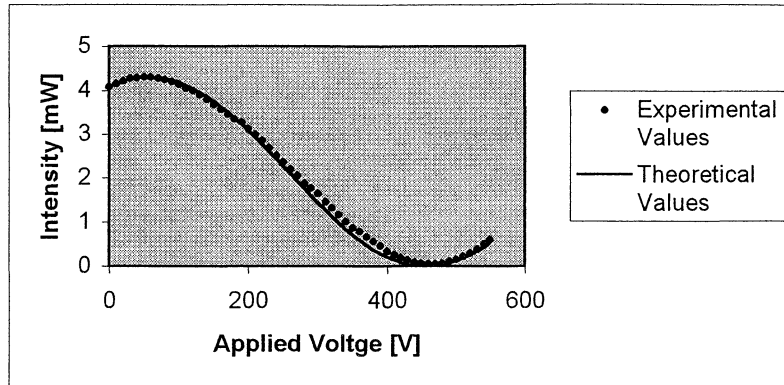


**Figure 5.4** The dependence of the intensity passing through the EOM on the applied voltage. Experimental values and theoretical values, using formula (5.7) with  $V_{\pi}=400$  V.

Comparing the theoretical value for  $V_{\pi}$  with the experimental value, shows that they lie close to each other, but the experimental value 400 V is somewhat larger than the calculated value 380 V. One possible reason could be that the crystal becomes warm during the scanning process, which involves applying several hundred Volts over a longer period of time to a small piece of crystal. As a crystal's indices of refraction change with temperature, the half-wave voltage could be changed if the crystal becomes warm.

The scanning for the first series was done very slowly and carefully and it involved 56 measurement points. Thus the whole measurement took more than 30 minutes.

Therefore another measurement was done where the scanning process was done faster. After adding appropriate constants to one of the curves, so that their maxima coincide, it is easier to compare them, see Figure 5.5. The slow series is more spread out than the fast series. For the fast series the half-wave voltage is smaller and lies around 380 V. In other words it is even closer to the calculated value than the result from the first measurement.

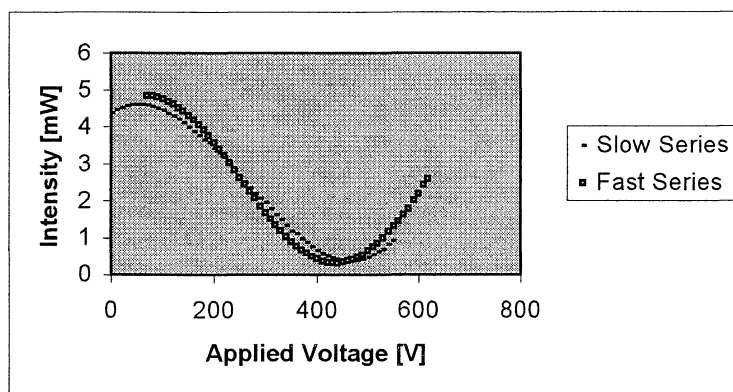


**Figure 5.5** Comparison between the slow and the fast measurement.

This measurement indicates that the temperature could be a possible reason for the difference in the two series. As the first series took more time the crystal should be warmer at the end of the first measurement than at the end of the second. Another reason could be space charge layers, which also could explain the observed hysteresis. When voltage is applied to the crystal's metal contacts, the existing surface states are influenced and change the crystal's band structure close to the interface. Therefore the voltage drop might be mainly across the surface and not across the bulk.

## 5.4 Improvements for the EOM

To get a better understanding of the temperature dependence of the indices of refraction, a thorough measurement should be done where the temperature can be controlled.

Thus a new set-up with temperature control for the electro-optic crystal was constructed. At the same time another improvement was done, making it possible to determine the speed with which the modulator could modulate.

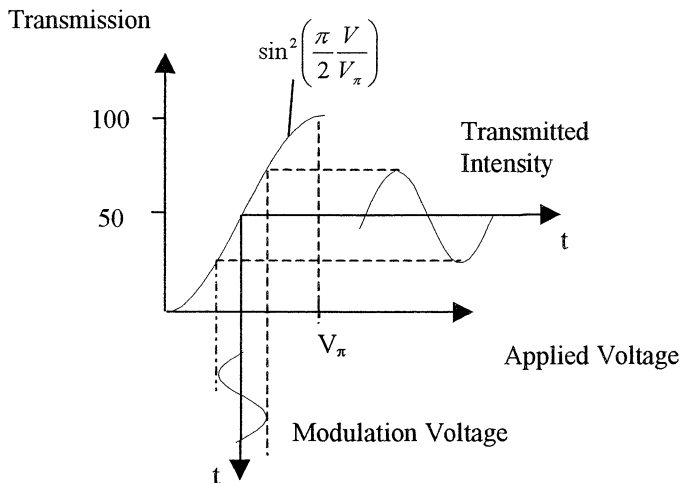


**Figure 5.6** Modulated amplitude's dependence on the applied voltage.

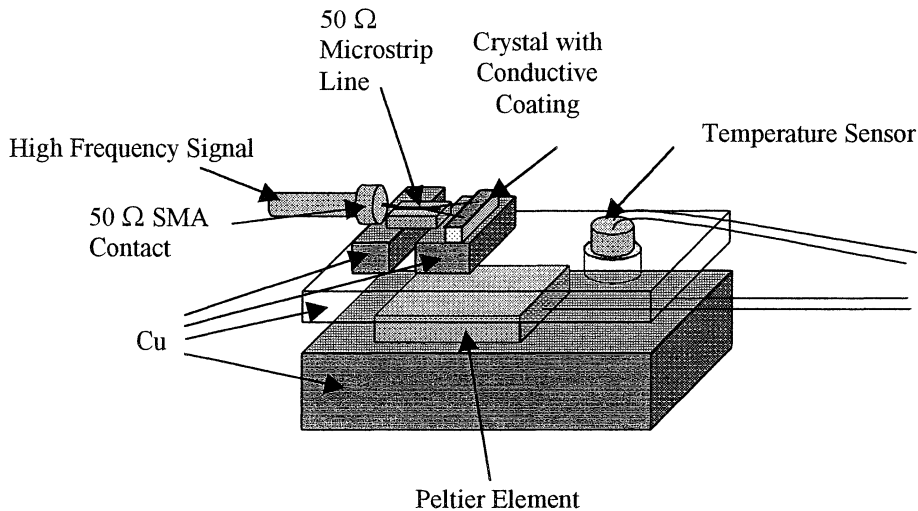
Figure 5.6 shows how the transmission depends on the voltage applied to the crystal. It is obvious that the slope is steepest at  $\frac{V_{\pi}}{2}$ . Thus the modulator will have the largest modulation coefficient, if the applied voltage is varied around  $V_{\pi/2}$ . In general a modulating radio frequency (rf) voltage is superimposed on the DC-bias voltage  $V_{\pi/2}$ .

## 6 The Modified EOM

### 6.1 Construction of the Modified EOM

A new electro-optic modulator had to be built, where it was possible both to measure and control the temperature of the crystal and to superimpose a rf voltage on top of the DC-bias voltage.

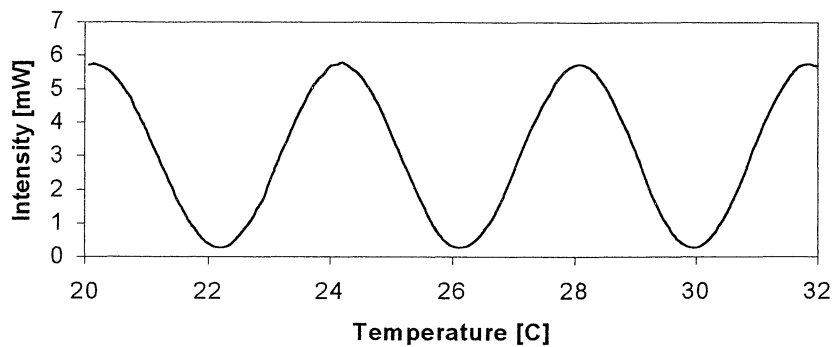
The temperature of the crystal could be determined by using a temperature sensor and in order to control the temperature, a Peltier-element had to be included in the construction. Moreover, the input signal from the high frequency cable was connected to the crystal via a 50  $\Omega$  SMA contact. This contact was connected to a 50  $\Omega$ -transmission line. It consists of an insulating, dielectric plate. The bottom is covered with copper and on the topside a short wire made of copper is situated. The wire has a diameter of approximately 200  $\mu\text{m}$  in order to diminish its inductance. The whole set-up can be seen in Figure 6.1.



**Figure 6.1** The new set-up for the electro-optic crystal and its contacts.

### 6.2 Temperature Measurement

In the first experiment no voltage was applied to the crystal. The temperature on the other hand was scanned from 20°C to 32°C and the intensity of the light passing through the whole set-up, including the two polarisers, the quarter-wave plate and the electro-optic crystal, was measured.



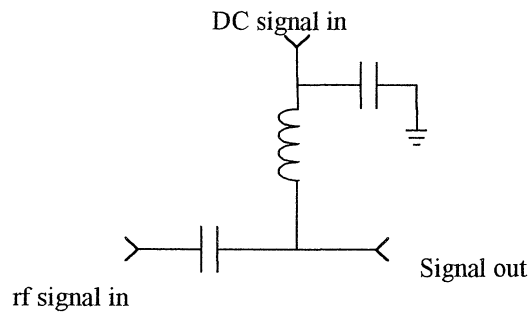
**Figure 6.2** The EOM changes from transmission to extinction mode, by changing the crystal's temperature 2°C.

Figure 6.2 shows clearly how sensitive the crystal is to changes in temperature. Heating or cooling the crystal only 2°C results in moving from a maximum to a minimum in transmission intensity. However, it is not clear, whether the temperature increased so much that it caused problems during the measurement in chapter 5.3, where the modulator's transmission was determined as a function of the applied voltage.

To avoid temperature problems, two electro-optic crystals, which are rotated 90° in relation to each other, could be placed in series in modulators. After having passed the first crystal the phase shift between the components is equal to  $\Gamma$ . In the second crystal the former y-component will travel along the z-axis and vice versa. If the crystals are exactly of the same size, all phase shifts, which are not due to the applied voltage, cancel. The phase shift due to the applied voltage, however, is doubled if the polarity of the voltage is switched on the second crystal in relation to the first.

### 6.3 High Frequency Measurement

The voltage applied to the crystal consists of two parts, a DC voltage, which is superimposed with a smaller modulated voltage. According to Figure 5.6 the DC voltage should be  $V_{\pi/2}$ , so that the modulator is working in the range where the transmission changes most quickly as a function of the applied voltage. In order to produce this combination of a high voltage superimposed with an - in comparison - low voltage modulated signal, a Bias Tee, HP-33150A, was used. The Bias Tee consists of an inductor and two capacitors, see Figure 6.3, and has a nominal transmission band from 0.1 to 18 GHz. One of the ports for the input signal is connected to the DC voltage and the other one is connected to the rf signal.



**Figure 6.3** The Bias Tee.

### 6.3.1 Determination of the Transfer Function

The rf signal is produced by a synthesiser, which can output single-frequency waves in the frequency range 1 MHz to 1024 MHz. As the effective voltage of this signal was less than 0.1 V, the signal had to be amplified. According to Figure 5.6 the EOM is most sensitive around  $V_{\pi/2}$ , but the result will be clearer when the modulated signal is larger than 1 V, due to a larger signal to noise ratio. Thus a 40 dB amplifier was included in the circuit. Unfortunately, the amplifier's ability to amplify a signal depends upon the frequency of the signal. Thus a measurement had to be done to register the amplification's dependence on the frequency. In order to measure the size of the amplified signal, an oscilloscope was included into the set-up. However, the input signal to our oscilloscope should not be higher than approximately  $\pm 30V$ , so the signal had to be attenuated by a 33 dB attenuator. This whole electric set-up can be seen in Figure 6.4.

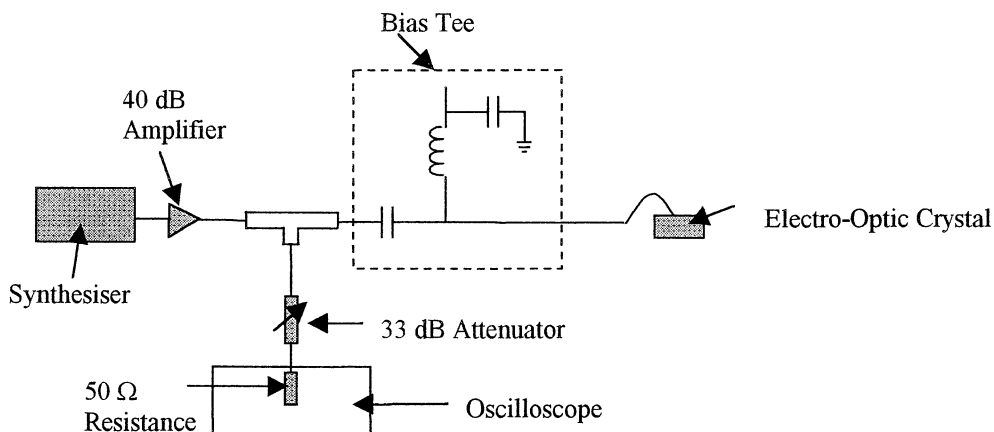


**Figure 6.4** Electric set-up for signal generation and the signal measurement.

The first step was thus to determine the frequency dependence of the transfer function for the signal, which passes through the amplifier, the Bias Tee and the attenuator. The transfer function of the attenuator is essentially flat up to 10 GHz, which means that it

does not affect the measurement and the frequency dependence is mostly due to the amplifier.

Thus the frequency was scanned from 1 MHz to 200 MHz and the signal was registered on the oscilloscope. After normalisation of the measurement series, the function is plotted in Figure 6.5.

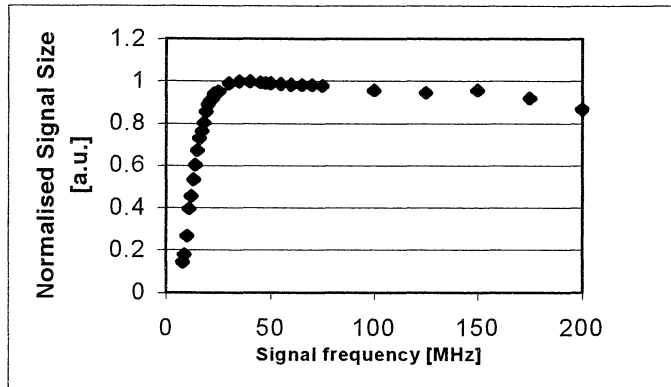


**Figure 6.5** The normalised transfer function for the amplifier, the Bias Tee and the attenuator.

The graph shows that certain - especially low - frequencies are not amplified as good as others. The low frequency cut-off is due to the blocking series capacitances in the amplifier and the Bias Tee. This transfer function has to be taken into consideration when the EOM's characteristics shall be determined.

### 6.3.2 Determination of the Crystal's Impedance

When a pulse is sent through a  $50 \Omega$  cable, which is terminated with a  $50 \Omega$  termination, nothing of the signal is reflected. If the termination on the other hand is infinity, the whole signal is reflected back and the registered signal on the oscilloscope is approximately twice as high as the original signal. Finally, if the termination is  $0 \Omega$ , the pulse is inverted and reflected back, which means that the signal on the oscilloscope is close to zero. Thus in order to examine whether the crystal's existence has some major influence on the signal detected by the oscilloscope, its impedance has to be determined as a function of frequency.

In general the impedance for a capacitor is given by  $Z_c = \frac{1}{\omega C_{crystal}}$ . This indicates that

the impedance decreases for high frequencies. Depending on the size of  $C_{crystal}$  it might even approach zero. If that is the case, the signal reaching the crystal will be smaller the higher the frequency is. This behaviour has to be considered when the modulator's ability to modulate light is determined.

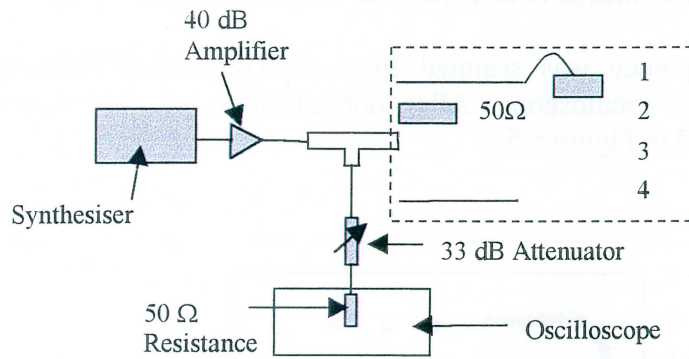


**Figure 6.6** The set-up for the series with different impedance terminations. The termination is 1. the high frequency cable and the electro-optic crystal, 2. a  $50\ \Omega$  termination, 3. nothing and 4. the high frequency cable.

In order to test this hypothesis, the Bias Tee from the set-up in Figure 6.4, was removed and four different series were measured, see Figure 6.6 and Figure 6.7. The first series shows the size of the signal, when the crystal is in its place. During the scanning of the second series, the cable connected to the crystal was removed and replaced by a  $50\ \Omega$  termination. The third series is the result from removing the  $50\ \Omega$  termination, which means having an infinite impedance. Finally, in the last series the cable leading to the crystal was put back in its position, but it was not connected to the crystal.

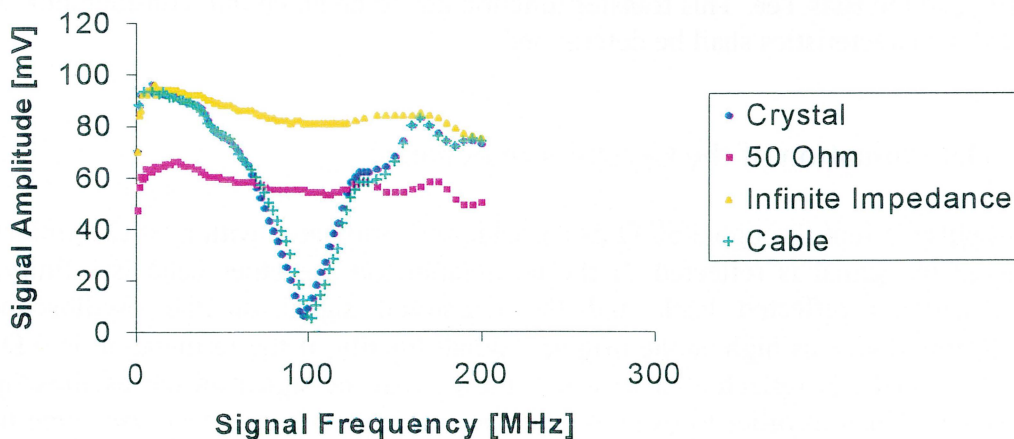


**Figure 6.7** The four series to determine the crystal's impedance.

From Figure 6.7 it is obvious that there is a resonance in the cable around 100 MHz when the signal is measured on the oscilloscope. However, this will not have any influence on the signal, which is applied to the crystal, during the future measurements. Thus, the crystal's impedance is close to infinity, because the curve representing the series with the crystal is close to the curve representing the series with infinite impedance.

This means that the crystal does not behave differently for high frequencies than for low frequencies. Moreover, it is clear that the crystal cannot receive a signal, which is close to zero because the crystal's impedance is not close to zero.

In principle, it is possible to calculate the capacitance for the RTP crystal, using the following equation for a plate capacitor

$$(6.1) \quad C = \epsilon_r \epsilon_0 \frac{A}{d}.$$

C is the crystal's capacitance, A the area of the top and bottom surface and d the thickness of the crystal. After having done the experiment, a value for RTP's dielectric constant was found in literature,  $\epsilon_r=13$ .<sup>9</sup> Using this value the capacitance can be determined to  $C = 1.15 \cdot 10^{-12} F$ . This shows that frequencies of several hundred MHz still result in impedances of over 1000  $\Omega$ .

### 6.3.3 The EOM's Ability to Modulate Light at Different Frequencies

After having determined the transfer function for the radio frequency signal, the intensity of the light passing through the EOM was measured as a function of frequency. A 1GHz detector (Thorlabs DET 210), which registered the laser's intensity, was connected to the oscilloscope. When the applied voltage on the electro-optic crystal, as explained earlier, is a DC signal of size  $V_{\pi/2}$  superimposed with a rf signal of a few Volts, the light's intensity is modulated at the rf frequency.

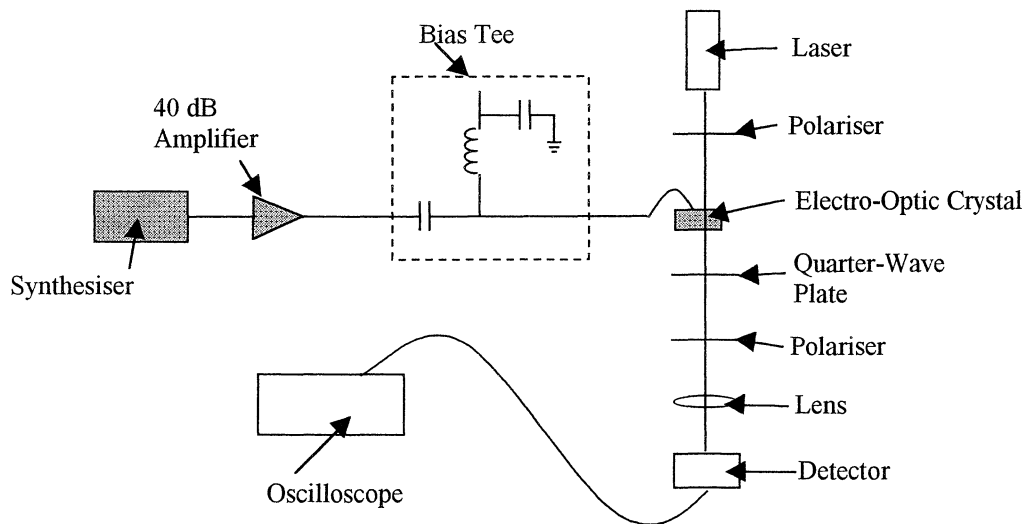


**Figure 6.8** The whole set-up for determining the modulator's speed.



In Figure 6.8 the whole set-up is shown, it includes the parts, which are needed for the generation of the modulation voltage and the equipment used to detect the modulated laser light.

The next step was to measure the amplitude of the modulated light for a range of frequencies. Thus the frequency of the rf signal was scanned from 1 to 200 MHz. At the same time the detector, which was connected to the oscilloscope, registered the intensity of the light passing through the modulator. The result is plotted in Figure 6.9.

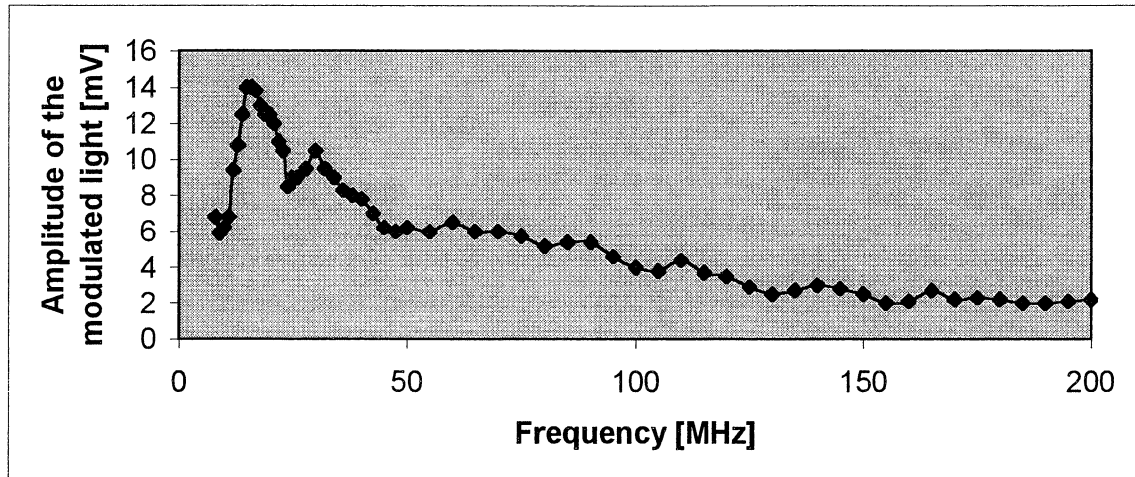
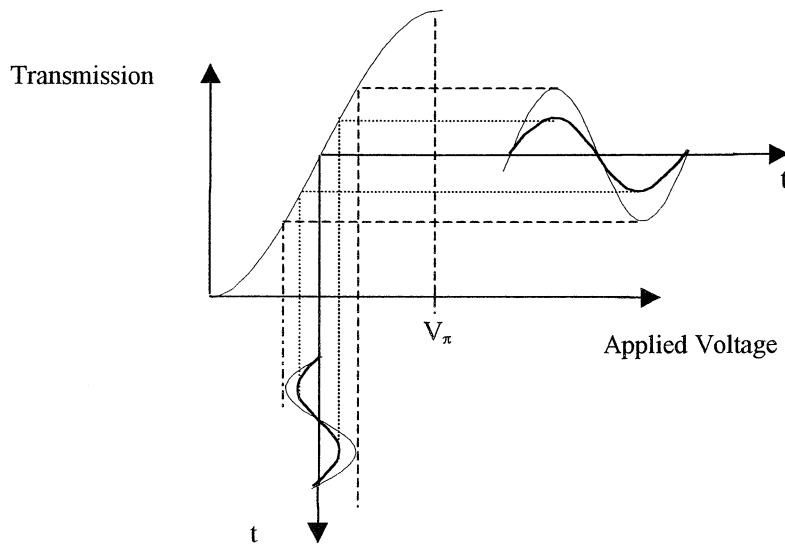


Figure 6.9 Amplitude of the modulated light as a function of frequency.

However, Figure 6.9 is not taking into account that the amplitude of the rf part of the voltage applied to the crystal is not the same for all frequencies. This means that the transfer function has to be included in the analysis of the modulator's ability to modulate light at different frequencies. Before the response of the EOM can be calibrated, the voltage on the crystal must be known. Due to the electro-optic crystal's capacitance and the connection's inductance the total impedance will depend on the frequency and thus the voltage on the crystal will vary. If the amplitude of the rf signal of the applied voltage decreases, the amplitude of the light modulation decreases as well. This can be seen in Figure 6.10.

As the relation between the applied voltage and the transmission is almost linear around  $V_{\pi/2}$ , one can say that if the applied voltage decreases by a factor of two, then the transmission also decreases by a factor of two.



**Figure 6.10** Detail of Figure 5.6. Decreasing the amplitude of the rf signal by a factor of two decreases the amplitude of the modulated light by a factor of two.

This means that in order to get a correct picture of the modulator's frequency dependence, the values in Figure 6.9 must be divided by the transfer function, which means by the values in Figure 6.5. The result is shown in a new graph, Figure 6.11.

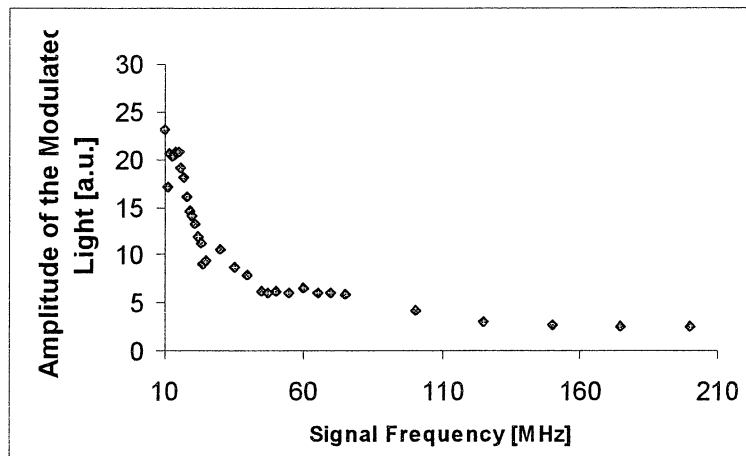


**Figure 6.11** The true amplitude of the modulated light as a function of frequency.

From Figure 6.11 it can be seen that although the transfer function is taken into consideration, the modulator seems to be working better for lower frequencies. In this case “better” refers to the contrast ratio the modulator can produce, because the higher the amplitude of the modulated light, the higher is the percentage of light, which can be blocked. One reason for this behaviour could be that the electro-optic coefficients change depending on the frequency of the applied voltage. In general, the values are larger for low frequencies than for high frequencies. A decreased value for  $r_c$  results in a higher half-wave voltage. Thus the curve representing the intensity, passing through the modulator, depending on the applied voltage is less compressed, which means it is less steep around  $V_{\pi/2}$ , where the modulator is run. Therefore the amplitude of the modulated light is smaller. However, no values, showing the frequency dependence of RTP’s electro-optic coefficients, could be found.

### 6.3.4 The High Speed EOM

Finally, Figure 6.12 and 6.13 show the light’s modulation at 100 MHz. In Figure 6.12 the applied voltage signal is approximately a sine wave, whereas the signal in Figure 6.13 is a pulse train intentionally produced by an overloaded amplifier. The second signal was used in order to examine the modulator’s response to irregular signals. With the available equipment it was impossible to get a square wave at 100 MHz.

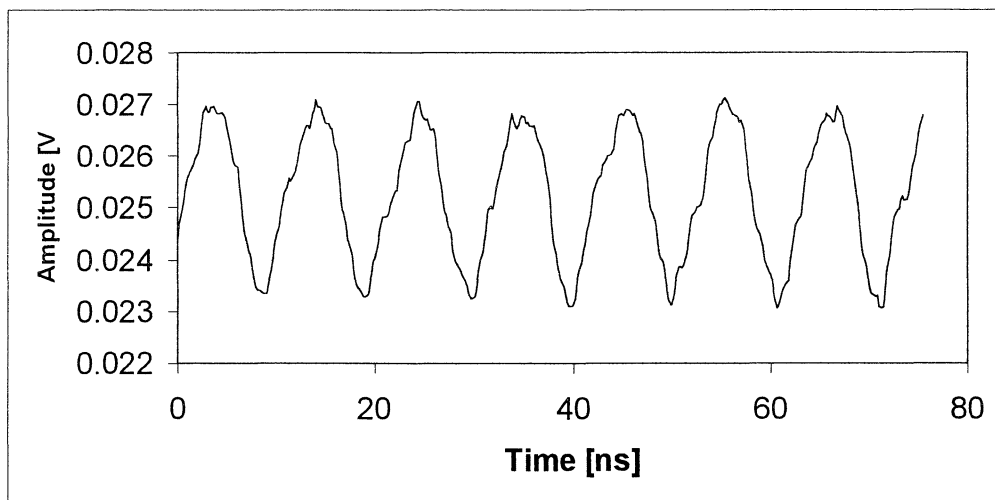


**Figure 6.12** The modulated intensity of the light passing through the modulator. The applied voltage is a sine wave with the frequency 100 MHz.

The voltage representing the minimum is approximately 85 % of the voltage at the maximum. In order to reach a higher contrast ratio the amplitude of the rf signal would have to be increased, but it is difficult to have a voltage, which is both modulated at a high frequency and has a large amplitude.

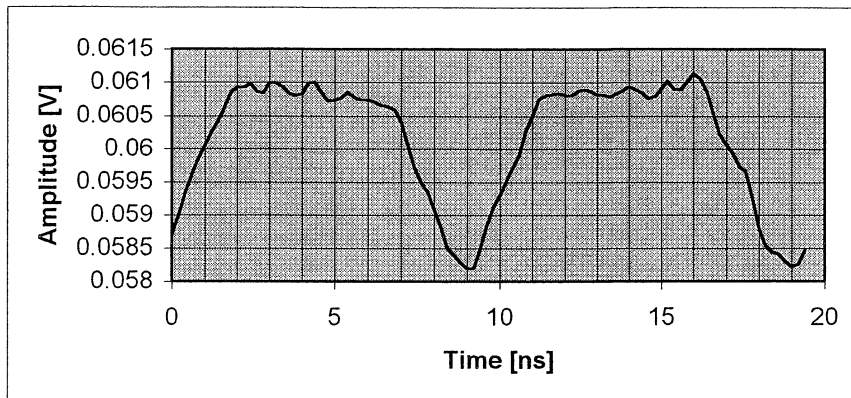


**Figure 6.13** The modulated intensity of the light passing through the modulator. The applied voltage is a pulse train intentionally produced by an overloaded amplifier with the frequency 100 MHz. The rise time of the modulator lies around 2 ns.

In Figure 6.13 it can be seen that the rise time for the modulator lies around 2 ns. Probably it is even lower because the applied voltage signal is not a square-wave and in addition to this, the detector has a rise time of 1 ns.

The last measurement, which should have been done, is to control the temperature at the same time as the EOM is used. Unfortunately, the temperature sensor cables, which are not shielded in this set-up, picked up the rf signal. Thus it was impossible to measure the temperature at the same time as the EOM was used.

## 6.4 Summary of EOMs

All in all this electro-optic modulator would be a solution for a laser TV because at the frequencies needed in a TV (32 MHz) it works as expected. At those frequencies the modulation of the light, which means the contrast ratio, is sufficiently high as well.

## 7 Summary

The aim with this thesis was to build a laser display, to examine different types of display techniques and to build a fast intensity modulator, which can be used for visible light.

As the first part of the work a projector, which can draw vector graphics, was constructed. It is possible to display geometric figures and text using this set-up. Moreover almost any figure can be displayed, once all the points making up the image have been saved on the computer or the flash card.

The restricting components in this set-up were the x-galvanometer and the connection between the computer and the servo cards. It was not possible to send as much data per second as needed in order to display complex images, which were stable. Moreover the scanners' maximum speed of 600 Hz reduced the complexity of the pictures, which could be displayed.

However, it should be possible to develop the vector graphics system into a scanning laser projector, if a polygon scanner replaces the x-galvanometer and some other adjustments are made. The Fraunhofer Institute in Germany is building polygon scanners, which are sufficiently fast for this application and which also have been tested for this purpose.

One of the other developments, which needs to be done, before a raster scanned system can be built, was to construct a fast intensity modulator. As the light used in a laser display will be visible a modulator for the visible range is needed. A modulator using an electro-optic crystal made of RTP was developed. This electro-optic modulator can modulate light at frequencies of several hundreds MHz, which is more than sufficient for the usage in a laser display unit.

- <sup>1</sup> Mool c. Gupta, *Handbook of Photonics*, CRC Press, 1996
- <sup>2</sup> <http://www.efg2.com/Lab/Graphics/Colors/Chromaticity.htm>
- <sup>3</sup> S. Kubota, M.Oka, J. Berger, *Prospects and approaches for laser color display based upon grating light valve technology*, Sony Corporation, Silicon Light Machines
- <sup>4</sup> Randall J. Knize, *Laser Television*, ERIP Recommendation #676, 1996
- <sup>5</sup> [http://cord.org/cm/leot/course04\\_mod07/mod04\\_07.htm](http://cord.org/cm/leot/course04_mod07/mod04_07.htm)
- <sup>6</sup> L.-T. Cheng, L. K. Cheng, J. D. Bierlein, *Linear and Nonlinear Optical Propertier of the Arsenate Isomorphs of KTP*, SPIE Proc vol 186, 43 (1993)
- <sup>7</sup> Eugene Hecht, *Optics*, Third Edition, Addison-Wesly, 1998, ISBN 0-201-30425-2
- <sup>8</sup> J.D. Bierlein, H. Vanherzeele, *J. Opt. Soc. Am B* 6, 622, 1989
- <sup>9</sup> <http://www.raicol.com/rtp.html>

Books and articles I have used for general information and understanding

1. Dennis Roddy, John Coolen, *Electronic Communications*, Second Edition, Reston Publishing Company, Inc, 1981, ISBN 0-8359-1631-6
2. Amnon Yariv, *Optical Electronics*, Third Edition, Holt-Sauders International Editions, 1985, ISBN 4-8337-0274-6
3. Eugene Hecht, *Optics*, Third Edition, Addison-Wesly, 1998, ISBN 0-201-30425-2
4. Hiroshi Nishihara, Masamitsu Haruna, Toshiaki Suhara, *Optical Integrated Circuits*, McGraw-Hill Book Company, 1987, ISBN 0-07-046092-2
5. <http://www.repairfaq.org/sam/crtfaq.htm>